Submitted to Nuclear Physics B;
also filed as a Ph.D. thesis

LBL-3022
Preprint

ANTIBARYON PRODUCTION AND HIGH ENERGY OSCILLATIONS

Joel Koplik

April 1974

Prepared for the U. S. Atomic Energy Commission
under Contract W-7405-ENG-48

DISCLAIMER

ANTIBARYON PRODUCTION AND HIGH ENERGY OSCILLATIONS*

Joel Koplik

Lawrence Berkeley Laboratory
University of California
Berkeley, California 94720

April 1974

Abstract

We employ multiperipheral models to investigate the proposal that the experimentally observed production of antibaryons can account for most or all of the rise in the pp total cross section at ISR energies. Our models support the proposal, and furthermore predict that this rise is the first part of a long-wavelength damped oscillation as a function of energy. We find that a variety of models accomodate the antibaryon effect, and show that these all lead to total cross sections consistent with present data and displaying an oscillation at higher energies. We attempt to understand the antibaryon cross section itself within the special case of the ABFST model, and find that the observed energy threshold emerges naturally, but that the predicted magnitude is somewhat small. The oscillations are simply parametrized in terms of complex Regge poles, and one of the models studied suggests that the leading complex pole be identified with the P'.

*Supported by the U. S. Atomic Energy Commission.

1. INTRODUCTION

A striking characteristic of recently obtained experimental results at high energy [1,2] is a tendency for hadronic cross sections to rise: the pp total cross section and most inclusive cross sections are observed to increase substantially with energy. While many explanations have been advanced for this phenomenon, we find it most plausible to attribute it to threshold effects. In the case of inclusive spectra, the cross section obviously must increase from zero, and one naturally expects that higher energies would be required to produce more massive particles copiously. Several detailed calculations [3], based on variants of the multiperipheral model, have lent support to this idea by qualitatively reproducing the experimental energy dependence of inclusive spectra. Basically, a "t_{min}" effect is responsible: hadronic scattering amplitudes are large only when momentum transfers are small, and if large masses are to be produced, simple kinematics requires the incident energy to be extremely large. Furthermore, once most inclusive cross sections are rising, it is not surprising that the total cross section rises as well. Our principal intention in this paper is to show that just such a multiperipheral threshold effect provides an understanding of the energy dependence of the total cross section.

Because of the multitude of particles and resonances that may occur in a high energy process, a realistic attempt to calculate a total cross section based on these ideas would require a morass of detail. We will avoid this by adopting the optimistic view that the rise in the total cross section may be understood in terms of the production of just one prominent, massive system. As noted by several authors [4-6], a likely candidate is the production of antibaryons. In fig. 1 we show

the experimental results for the integrated antibaryon* inclusive cross section as a function of energy [7]. The key features of this curve are its large magnitude and the approximate threshold at $s \approx 150$ GeV^2. The latter value is in rough agreement with the energy at which the pp cross section probably begins to rise. While our analysis will attempt to attribute all of the increase in the total cross section to antibaryon production, we will be making several approximations and using parameters that are not known accurately, so the possibility of other mechanisms contributing is not ruled out. However, our results will strongly support the view that at least a large part of the increase is due to antibaryons.

A byproduct of this analysis is the prediction of long-wavelength damped oscillations in the total cross section as a function of energy [8]. These occur because the effective thresholds for the production of various numbers of antibaryons develop an approximate logarithmic spacing, due to the aforementioned t_{min} effect, and the strong energy dependence of these partial cross sections reflects itself in the total [9]. Since these oscillations are perhaps the most unusual feature of our discussion, in this paper we pay particular attention to possible mitigating factors that might suppress them. We will conclude that the antibaryon-induced oscillations are quite persistent and stable under variation of the model used to obtain them.

Our arguments will be entirely within the context of the multiperipheral model, and we should explain how this model is used here.

---

*This curve is taken from ref. [6]; these authors refer to it as the antinucleon cross section, but the arrangement of apparatus at the ISR is such that the decay products of antihyperons are included. We will also assume throughout this paper that to a good approximation at these energies, at most one antibaryon appears per event.

The basic assumption is that the bulk of the total cross section can be attributed to multiparticle events occurring at small momentum transfers, and that these can be described reasonably by a model employing repetition of a small number of particle clusters in the t-channel. Most features of observed data are consistent with this assumption [10]. It will be evident from the particular models we study that our conclusions are rather insensitive to the specific implementation of the multiperipheral idea. For the most part we will use models that have been reduced to a "one-dimensional" form by averaging over momentum transfer. This provides a great simplification, and we shall argue that no essential physics is lost thereby. The main disadvantage of this approximation is that it precludes a corresponding treatment of inclusive cross sections.*

In section 2 of this paper we use the ABFST [12] or pion-exchange multiperipheral model to motivate some of the later discussion and then to estimate the relevant energy thresholds. The latter are found to be in rough agreement with experiment. We also use this model for a crude estimate of the magnitude of the antibaryon cross section: the result is surprisingly large, but somewhat smaller than experiment indicates. An interpretation of the large size of the antibaryon cross section in terms of resonances induced by the long-range pion-exchange force is given. Section 3 presents the derivation of the kind of model used in this paper, and successfully applies the simplest version to pp data [6]. A discussion of oscillations is given and the role of complex Regge poles elaborated. In each of the next three sections the simple model is made more realistic in one direction at a time. Section 4

*Further remarks on this subject are in section 4; a discussion of total and inclusive cross sections using a smooth t-dependence may be found in ref. [11].

discusses the effect of a smooth antibaryon threshold and that of thresholds for the production of other particles. Section 5 treats a more realistic antibaryon kernel, and in section 6 we discuss diffractive effects. The general features of the total cross section are found to be the same as in the simplest case. We present some final remarks in section 7, and an Appendix contains a more detailed discussion of the model used for our treatment of diffractive scattering.

2. ESTIMATES BASED ON THE ABFST MODEL

The first question we wish to examine is whether the observed antibaryon cross section can be understood in terms of familiar phenomena and, in particular, whether it is consistent with the multiperipheral ideas to be used in this paper. Rather than the detailed shape of fig. 1, whose fitting would require considerable input of information, we concentrate in this section on the location of the approximate threshold and the magnitude of the cross section. For the purpose of making order-of-magnitude estimates, we adopt the ABFST multiperipheral model [12], based on repeated pion exchange, which allows us to compute high energy quantities from known, low-energy pion scattering information. While this model is known to be numerically deficient, in that the pion component alone is too small to account for high energy data [13], the general behavior it predicts has been verified and we shall assume no gross error is made if we scale the size of the pion-exchange kernel upward, as described below.

We begin by describing the ABFST model, using the notation of ref. [13]. The contribution of N+2 pion-produced clusters of particles to the absorptive part of the a-b forward elastic scattering amplitude is depicted in fig. 2.1, and given by

$$A_{ab}^{(N)}(\eta) = \frac{1}{\sinh \eta} \int ds_a\, ds_1 \cdots ds_N\, ds_b\, dt_0 \cdots dt_N$$

$$\times G_{a\pi}(s_a ; t_0)\, S(t_0)\, G_{\pi\pi}(s_1; t_0, t_1)\, S(t_1)$$

$$\cdots G_{\pi\pi}(s_N; t_{N-1}, t_N)\, S(t_N)\, G_{\pi b}(s_b; t_N) \qquad (2.1)$$

$$\times \frac{1}{N!} (\eta - q_a - q_1 - \cdots - q_N - q_b)^N \theta(\eta - q_a - \cdots - q_b),$$

where

$$\cosh \eta = \frac{s - m_a^2 - m_b^2}{2 m_a m_b}, \qquad (2.2a)$$

$$\sinh q_a = \frac{s_a - m_a^2 - t_0}{2 m_a \sqrt{-t_0}}, \qquad (2.2b)$$

similarly for $\sinh q_b$, and

$$\cosh q_i = \frac{s_i - t_{i-1} - t_i}{2\sqrt{t_{i-1} t_i}}. \qquad (2.2c)$$

The s_i and t_i are the subenergies and momentum transfers shown in the figure, $S(t)$ is a pion propagator and $G_{\pi\pi}(s;t,t')$ is proportional to the cross section for off-shell pions of squared-masses t and t' to produce a particle cluster of subenergy s_i, integrated over the internal variables of the cluster. $G_{\pi\pi}$ will be referred to in the following as the π-π "kernel" for the cluster in question. For the present we will assume these are "low"-subenergy kernels, in that a possible diffractive tail arising from P and P' exchange is absent. Diffractive effects would not alter the present estimates, and their inclusion will be discussed in section 6. Furthermore, since the momentum transfers involved are small (we are, after all, studying the multiperipheral model), we will assume these cross sections are given by their

"on-shell" or physical values. Finally, in formula (2.1) the q's are Lorentz boost angles for the transformation between standard reference frames [14] associated with particles a and b and the various pions, and the step-function (which essentially expresses energy conservation) requires that the overall boost η between the a and b standard frames be at least as large as the sum of the individual boosts across each cluster.

Within this model, antibaryons may be produced in a pp collision through the appearance of either of the clusters shown in fig. 2.2a or b, respectively at the ends or in the middle of the multiperipheral chain. The effect of cluster involving particles in addition to the baryons will be considered later. Now the cross section corresponding to fig. 2.2a is small (it has never been measured) and so we neglect it. This is in agreement with the experimental fact that the antibaryon inclusive cross section falls rapidly near the ends of a rapidity plot [7], whereas the products of cluster 2.2a would populate just this region. The internally-appearing cluster, fig. 2.2b, has however a substantial cross section, and in fig. 2.3 we show the experimental results for the case $\pi^+\pi^- \to p\bar{p}$ [15].*

We first show how the smallness of momentum transfers implies the observed energy threshold for this cluster. For simplicity fig. 2.3 is approximated by a delta-function peak at a mass M = 2.1 GeV, and we assume that the amplitude is important only for momentum transfers

*The reference quoted gives the result of a Chew-Low extrapolation in the reaction $\pi^- p \to (p\bar{p})n$, and notes that this agrees well with the cross section as determined from the inverse reaction $p\bar{p} \to \pi^+\pi^-$ and detailed balance. This agreement argues against the possible presence of important corrections to pion-pole dominance.

falling within a cutoff T such that

$$-t < T << M^2$$

and negligible outside this range. The first assumption is surely adequate for estimating a threshold, while the assumption of a sharp cutoff in momentum transfer, although unrealistic, is justified in section 4 and by the work of ref. [11]. From eq. (2.2c) we see that the boost q across the baryon-antibaryon cluster is bounded by

$$\cosh q \gtrsim \frac{M^2}{2T}$$

or

$$q \gtrsim \log \frac{M^2}{T} . \qquad (2.3)$$

Any additional $\pi\pi \to B\bar{B}$ cluster appearing in the chain then requires an internal boost of at least this value, and from the step-function in eq. (2.1) we see that each additional antibaryon cluster requires an increment of at least $\log(M^2/T)$ in rapidity, η.

The overall energy threshold for antibaryon production is then that of fig. 2.4, where we expect that p^*, the particle-cluster appearing at the ends, is either a nucleon or Δ-resonance. In the first case T is extremely small: it can be estimated from np backward elastic scattering which is dominated by pion exchange and whose cross section has been measured to be

$$\frac{d\sigma}{du} \propto s^{-2} e^{bu}$$

with $b \sim 30\text{-}100\ \text{GeV}^{-2}$ [16]. If we assume that the t-damping is the same for fig. 2.4, then from eq. (2.2b) the end boosts are negligible:

$$\sinh q_p = \sqrt{-t_0}/2m_p \lesssim \sqrt{T}/2m_p << 1$$

and the threshold requirement is $\eta \gtrsim q_{B\bar{B}}$. The observed threshold (fig. 1) would correspond to $T = 0.03\ \text{GeV}^2$, a value quite consistent

with the np data, although because of the inherent uncertainty in this procedure a clean prediction cannot be made. For the case of a $\Delta(1236)$ being produced at the end, q_p is no longer negligible. However, using eqs. (2.2) we find that the observed antibaryon threshold corresponds to $T = 0.20\ \text{GeV}^2$, again a value consistent with data obtained from pion-pole extrapolation experiments [17]. Thus the observed antibaryon threshold is in agreement with the ABFST model.

We now turn to estimating the magnitude of the antibaryon cross section. The precise connection between the cross section for $\pi\pi \to B\bar{B}$ and antibaryon production in a pp collision is not immediately obvious and will be discussed in the following sections, but from (2.1) we see that some sort of weighted integral of the former over energy is required. Much of out later discussion will employ a narrow resonance approximation for the antibaryon kernel, so it suffices to consider just the simple integral—the area under the curve in fig. 2.3—since any moment of this cross section is then simply related to its area. To take into account other charge states of the pions and often types of baryon we multiply the area under fig. 2.3 by 3×8. Strictly speaking, of course, we should use the individual cross sections together with the isospin and SU(3) crossing matrices, but this information is not available and the crude procedure should be adequate for an order of magnitude estimate. We should also include the possibility of producing unstable baryon-antibaryon pairs (such as $\Delta\bar{\Delta}$) which then decay, and to allow for this we assume exact SU(6) symmetry and replace the factor of 8 (for the baryon octet) by 28*. In this way we find that the net integrated

*This number is obtained by attributing half the $p\bar{p}$ cross section to each spin state, and assuming that all members of the $\underline{56}$ representation of SU(6) contribute equally. Needless to say, this is a generous estimate.

$\pi\pi \to B\bar{B}$ cross section is roughly one-third of the integrated $\pi\pi \to$ mesons cross section, where for the latter we use the estimates of ref. [13]. If the pion-exchange model were quantitatively correct the integrated $\pi\pi \to$ mesons cross section would account for most of the total cross section, but in fact it falls short by a factor of 3-4. We assume, as described above, that a fair approximation to real life is obtained by scaling all pion-exchange results upward by this factor. Thus the integrated antibaryon-producing kernel is estimated to have roughly one-third the strength of the meson-producing kernel which generates most of the cross section. Although this is a large fraction, we shall see later that it is still too small to account for the experimental results.

At first glance it is rather surprising that the antibaryon cross section is so large; the fact itself is sufficient for the other arguments in this paper, but we may offer a qualitative explanation as follows. The two-baryon system is somewhat distinguished in that it allows a long-range one-pion exchange force, which is prevented by quantum number considerations from appearing in many two-meson systems (e.g., $\pi\pi$, $K\bar{K}$, $\rho\rho$). It was shown some time ago by Ball and Chew [18] that a simple non-relativistic treatment of this force in the two-nucleon system provides an understanding of the large cross section for low-energy $p\bar{p}$ scattering as compared to pp. This is basically a low-kinetic-energy classical nuclear physics situation and, as is the case there, it is natural to think of it in terms of a number of overlapping resonances near threshold. If, therefore, we assume that the $B\bar{B}$ system near threshold is dominated by an unusual accumulation of resonances there, the large size of the antibaryon kernel is not very surprising.

The resonance point of view provides us with the means for

remedying an important omission in the preceding analysis. We have ignored the fact that a $B\bar{B}$ system has a strong tendency to annihilate to many pions; in other words, final-state interactions within the $B\bar{B}$ system have been omitted.* We should add a term to the multiperipheral kernel corresponding to $\pi\pi \to$ ($B\bar{B}$ resonance) $\to$ many pions. With some simplifications, the assumption that the $B\bar{B}$ system is dominated by resonances at low energy allows an estimate of this effect. The key is the factorization property of a resonance pole residue.

We make the approximation of supposing there is only one spin-0 resonance in question, and that we may approximate the interaction of the $B\bar{B}$ and many-pion states involved as the quasi-two-body scattering of spinless particles. The cross section for $a \to b$ in a single partial wave is then

$$\sigma_{ba}^{L} = \frac{4\pi}{k_a^2}(2L+1)\left|\frac{S_{ba}^{L} - \delta_{ba}}{2i}\right|^2,$$

where k_a is the center-of-mass momentum of state a. Specializing to the s-wave, and extracting the threshold behavior according to

$$S_{ba}^{0} - \delta_{ba} = \sqrt{k_b k_a}\, T_{ba},$$

we have

$$\sigma_{ba} = \pi \frac{k_b}{k_a}\left|T_{ba}\right|^2. \tag{2.4}$$

Now for the $p\bar{p}$ system, we write

$$T_{ba} = g_b g_a f(k_p), \tag{2.5}$$

where $k_p^2 = s/4 - m_p^2$ and $f(k_p)$ is a function with an appropriate resonance peak—a Breit-Wigner form, for example. If the peak is located somewhere near threshold, this will give $\sigma(\pi\pi \to p\bar{p})$ roughly the shape

*This point has been stressed by Einhorn and Nussinov [19].

of fig. 2.3. Then from equations (2.4) and (2.5), the relative probability of this resonance decaying to many pions compared to that for a $p\bar{p}$ pair is

$$\frac{\sum_n k_{n\pi}\, g_{n\pi}^2}{k_p\, g_p^2} = \frac{\sigma\,(p\bar{p}\ \text{annihilation})}{\sigma\,(p\bar{p}\ \text{elastic})} \approx 2.0,$$

where the numerical value quoted is obtained from low-energy data [16]. Assuming the same proportionality holds for other baryons, our previous estimate of the "antibaryon" kernel strength should be tripled to take into account this pion production.

3. THE TOTAL CROSS SECTION

With both theory and experiment agreeing upon the existence of an important component of the multiperipheral kernel associated with antibaryon production, we proceed to calculate its effects on the total cross section. In the remainder of this paper we shall employ a "one-dimensional" approximation in which momentum transfers have been averaged over, leading to amplitudes depending only on rapidity,* but with the relevant (sharp) peripheral thresholds retained. This simplifies our arguments considerably, and it is shown in section 4 and ref. [11] that a more careful treatment leads to similar results.

We will begin by discussing the simplest possible model which exhibits the threshold effects of interest [6, 9], and then go on to more realistic examples. Consider a reaction in which particles a and b produce N+2 clusters of particles which may include mesons or a baryon-antibaryon pair. We assume the amplitude may be approximated by repeated Reggeon or pion exchange. If we square this amplitude and integrate over phase space, we find fig. 3.1 for the (N+2)-cluster

*Such models are discussed by DeTar [20].

contribution to the forward a-b absorptive part, where an ordering in rapidity is implied. We denote the overall rapidity by η, the rapidity intervals across the end clusters by $x_{a,b}$ and across the internal clusters by x_i, and the rapidities across the Reggeons by y_i. Then

$$A_{ab}^{(N)}(\eta) = \int_0^\eta dx_a\, dy_0\, dx_1\, dy_1 \cdots dx_N dy_N\, dx_b$$

$$\times \delta(\eta - x_a - x_b - \Sigma x_i - \Sigma y_i)\, G_a(x_a) S(y_0) \qquad (3.1)$$

$$\times G(x_1)\, S(y_1) \cdots S(y_N)\, G_b(x_b),$$

where $S(y)$ is a Reggeon propagator for the sides of the ladder, and $G_{a,b}(x_{a,b})$ and $G(x)$ are kernels in the sense of the previous section and are proportional to the contribution of a cluster of rapidity interval x to the appropriate Reggeon absorptive part.

It will be trivial to solve for the full absorptive part,

$$A_{ab}(\eta) \equiv \sum_{N=0}^{\infty} A_{ab}^{(N)}(\eta), \qquad (3.2)$$

once we obtain an integral equation for it. To this end, we define a "one-sided" absorptive part $F_b^{(N)}$ by extracting the left-hand cluster and propagator from $A_{ab}^{(N)}$; write

$$A_{ab}^{(N)}(\eta) = \int_0^\eta dx\, dy\, G_a(x)\, S(y)\, F_b^{(N)}(\eta - x - y). \qquad (3.3)$$

Then $F_b^{(N)}$ obviously satisfies the recursion relation

$$F_b^{(N)}(Y) = \int_0^Y dx\, dy\, G(x)\, S(y)\, F_b^{(N-1)}(Y - x - y),$$

and summing over N as in (3.2) we have

$$F_b(Y) = F_b^{(0)}(Y) + \int_0^Y dx\, dy\, G(x)\, S(y)\, F_b(Y - x - y), \qquad (3.4)$$

where

$$F_b^{(0)}(Y) = G_b(Y) . \tag{3.5}$$

Taking a Laplace transform

$$F_b(J) = \int_0^\infty dY\, e^{-JY} F_b(Y), \tag{3.6}$$

and noting that (3.3) is a convolution integral, (3.4) becomes

$$F_b(J) = F_b^{(0)}(J) + G(J)\, S(J)\, F_b(J) \tag{3.7}$$

Thus from (3.2) and (3.3)

$$A_{ab}(J) = G_a(J)\, S(J)\, F_b(J)$$

$$= \frac{G_a(J)\, S(J)\, G_b(J)}{1 - G(J)S(J)} . \tag{3.8}$$

Since we will be making much use of equations of this type, it is perhaps worthwhile to sketch an alternative derivation, which will also clarify its relation to the ABFST model. We start from formula (2.1) and insert the identity

$$\frac{1}{N!} x^N \theta(x) = \frac{1}{2\pi i} \int_c dJ\, \frac{e^{(J+1)x}}{(J+1)^{N+1}}, \tag{2.1}$$

where c runs parallel to the imaginary J axis to the right of J = - 1. This gives

$$A_{ab}^{(N)}(\eta) = \frac{1}{2\pi i} \int_c dJ\, \frac{e^{(J+1)\eta}}{\sinh \eta} \int dt_0 \cdots dt_N$$

$$\times \tilde{G}_{a\pi}(J; t_0)\, S(t_0)\, \tilde{G}_{\pi\pi}(J; t_0, t_1) \cdots$$

$$S(t_N)\, \tilde{G}_{\pi b}(J; t_N), \tag{3.a}$$

where

$$\tilde{G}_{\pi\pi}(J; t, t') = \frac{1}{J+1} \int ds\, G_{\pi\pi}(s; t, t')\, e^{(J+1)q(s; t, t')}$$

and similarly for $\tilde{G}_{\pi a, b}$. We then approximate the t integrals by a single average value of momentum transfer:

$$S(t) = \frac{c}{T^2}\, \delta(t + T) ,$$

where c is a dimensionless constant and $\langle t \rangle = - T$. As before, T is assumed to be much less than the important masses appearing in the G's, which from (2.2c) leads to

$$e^{q(s; T, T)} \approx \frac{s}{T} .$$

Equation (3.9) then becomes

$$A_{ab}^{(N)}(\eta) = \frac{1}{2\pi i} \int_c dJ\, \frac{e^{(J+1)\eta}}{\sinh \eta} \left\{ G_{a\pi}(J)\, S(J) \right.$$

$$\left. \times G_{\pi\pi}(J) \cdots S(J)\, G_{\pi b}(J) \right\} , \tag{3.10}$$

where

$$G_{\pi\pi}(J) = \int ds\; s^{-J-1}\, G_{\pi\pi}(s; T, T),$$

similarly for $G_{\pi a, b}$, and

$$S(J) = \frac{c}{J+1}\, T^J .$$

If we now sum over N, the quantity in braces is precisely (3.8), and finally we note that for not-too-small values of η the J integral in (3.10) is just the inverse Laplace transform.

Our next step is to choose the functions G and S and examine the resulting cross section. For the cluster at the ends of the chain we assume a single narrow resonance:

$$G_a(x_a) = g_a\,\delta(x_a - \Delta_a)\,, \tag{3.11a}$$

where g_a is the integrated strength of this resonance and Δ_a the rapidity it spans. The internal cluster may be either a meson or a $B\bar{B}$ system, and we write

$$G(x) = g_M\,\delta(x) + g_B\,\delta(x - \Delta_B). \tag{3.11b}$$

The meson and baryon clusters have strengths g_M and g_B and rapidity intervals 0 and Δ_B, respectively. From the earlier discussion, Δ_B should be identified as the internal threshold for a $B\bar{B}$ system, and $\Delta_{a,b}$ as the corresponding thresholds for the ends of the chain. We have, for the moment, assumed the meson rapidity interval is negligible. For the propagator we write

$$S(y) = e^{\beta y}, \tag{3.12}$$

where β is to be interpreted as $2\bar{\alpha}-1$, $\bar{\alpha}$ being the average spin of the object exchanged along the multiperipheral chain. In the pion exchange case, for example, $\beta = -1$. Strictly speaking, an overall constant should appear in (3.12), but we choose to absorb it into the G's. Laplace transforming (3.11) and (3.12) and substituting into (3.8), we obtain, finally,

$$A_{ab}(J) = \frac{g_a g_b\, e^{-(\Delta_a+\Delta_b)J}}{J-\alpha_0 - g_B\, e^{-\Delta_B J}}\,, \tag{3.13}$$

where

$$\alpha_0 \equiv \beta + g_M\,. \tag{3.14}$$

We now consider the cross section resulting from (3.13). First suppose there is no production of $B\bar{B}$ pairs, a situation which corresponds to $g_B = 0$. If we invert the Laplace transform according to

$$A(\eta) = \frac{1}{2\pi i}\int_{c-i\infty}^{c+i\infty} dJ\, e^{J\eta} A(J) \tag{3.15}$$

where c is to the right of the singularities of $A(J)$, we find

$$A_{ab}(\eta)\Big|_{g_B=0} = g_a g_b\, e^{\alpha_0(\eta-\Delta_a-\Delta_b)}, \tag{3.16}$$

so the meson clusters alone have generated a Regge pole at α_0. For $g_B \neq 0$, $A(J)$ has the set of poles shown in fig. 3.2: a real pole to the right of α_0 plus an infinite sequence of complex poles, together with their complex conjugate pairs (not shown). The contribution of such a complex pole pair at $\alpha = \alpha_R + i\alpha_I$ to $A(\eta)$ is

$$r\, e^{\alpha\eta} + r^* e^{\alpha^*\eta}$$

$$= 2\,|r|\, e^{\alpha_R\eta}\cos[\alpha_I\eta + \arg(r)]\,, \tag{3.17}$$

which is an oscillating function. Since α_R is always below the leading real pole, the oscillations are damped. The oscillations have the effect of reproducing the variation with energy of the total cross section that is associated with the threshold structure of the partial cross sections for various numbers of antibaryons. The latter quantities can be found by expanding the denominator of (3.13) in powers of g_B before inverting the transform [or from direct integration of (3.1)]. The result is

$$A_{ab}(\eta) = g_a g_b\, e^{\alpha_0(\eta-\Delta_a-\Delta_b)} \sum_{n=0}^{\infty} \frac{1}{n!}\left[g_B\, e^{-\Delta_B\alpha_0}\right]^n \times (\eta-\Delta_a-\Delta_b-n\Delta_B)^n\,\theta(\eta-\Delta_a-\Delta_b-n\Delta_B), \tag{3.18}$$

where the nth term represents the production of n $B\bar{B}$ pairs.

To relate this model to pp scattering and provide a numerical illustration of these ideas, we can choose the parameters involved in the following way: In section 2 we obtained two different estimates for the thresholds Δ_p and Δ_B, depending on whether the end cluster was a nucleon or a Δ-resonance, but both gave an over-all threshold

$$2\Delta_p + \Delta_B \approx 5.0 .$$

For simplicity we will just average the two alternatives, and this leads to $\Delta_p = 0.5$ and $\Delta_B = 4.0$. From the separate terms in (3.18), we can relate g_B to the slope of the antibaryon cross section at threshold. If σ_n is the partial cross section for n $B\bar{B}$ pairs, then

$$R_B \equiv \frac{1}{\sigma_0}\frac{d\sigma_1}{d\eta}\bigg|_{\eta=2\Delta_p+\Delta_B} = g_B e^{-\alpha_0\Delta_B}. \qquad (3.19)$$

Using the data shown in fig. 1, and taking into account the fact that the antibaryon kernel has been estimated to have roughly 3 times this strength due to additional pion production (section 2), we obtain $R_B \approx 0.3$. The Froissart bound requires that the Pomeron intercept in the model—the position of the leading (real) pole of (3.13)—not exceed 1. If we allow it to attain this value, which assumes that no other important clusters will apear at still higher energies, we can determine α_0. By requiring (3.10) to develop a pole at J = 1, we see that α_0 is the solution of the transcendental equation

$$1 - \alpha_0 - \left[g_B e^{-\Delta_B\alpha_0}\right] e^{-\Delta_B(1-\alpha_0)} = 0, \qquad (3.20)$$

and with the values quoted above we obtain $\alpha_0 = 0.84$. The leading complex poles are then found to occur at $J = 0.50 \pm 1.1i$ and $0.29 \pm 2.7i$.

In fig. 3.3 we show the cross section resulting from this parametrization. The solid line is the exact cross section obtained from

(3.18), while the dotted lines labeled by values of n are the partial cross sections. The dashed line is the asymptotic expansion obtained from the real pole plus the leading complex pair; it provides a very good approximation to the exact result if η is not too small.

Before comparing this curve with experiment, a preliminary remark is required. In formulating multiperipheral equations, one always diagonalizes with respect to t-channel quantum numbers such as angular momentum, isospin, and signature. In particular, since we are here concerned with high-energy scattering and the Pomeron, the part of the amplitude with even t-channel signature is involved. This means we have really constructed a model for the sum of pp and $p\bar{p}$ total cross sections. Unfortunately, very high energy $p\bar{p}$ scattering measurements do not exist, and we are forced to extrapolate this amplitude. We shall suppose that for all energies of interest that

$$\sigma^{tot}_{p\bar{p}}(s) = \sigma^{tot}_{pp}(s) + cs^{-1/2}, \qquad (3.21)$$

where c is chosen to fit the available data at lower energy. With this prescription "experiment" is then compared to this model in fig. 3.4, and the agreement is satisfactory. As a byproduct of studying the even signature amplitude, we can immediately obtain the full (forward) amplitude from its absorptive part by inserting the appropriate Regge signature factors:

$$F(\eta, 0) = \sum_\alpha - \frac{1 + e^{-i\pi\alpha}}{\sin\pi\alpha} r_\alpha e^{\alpha\eta} , \qquad (3.22)$$

where the sum runs over the Regge poles of (3.13), and the r_α are pole residues. In fig. 3.5 we plot the ratio of real to imaginary part. This shows the same oscillations as σ^{tot}, but shifted in phase by 90°.

From the figures we see that damped oscillations in various observable quantities are predicted byt his model, and one is immediately led to ask if these are observable. This of course depends on the period of oscillation; in the model just presented, the period is 4 units of rapidity, and a modest increase in ISR capabilities would push the range of avilable energies past the maximum. Unfortunately, our estimate of the period has been crude and might be increased in either of two ways: the value of the momentum transfer cutoff might be smaller than we have supposed, or the effective mass of the $B\bar{B}$ system might be larger. In particular, within the second category, we could have allowed the $B\bar{B}$ system to have an unlimited mass as given by baryon Regge exchange (fig. 3.6). In section 5 we will discuss a model which includes this effect, and a substantial increase in oscillation period will result.

4. MORE REALISTIC KERNELS

In the last section we saw that the incorporation of antibaryon production into a very simple model led to a threshold increase and subsequent oscillation of the total cross section, and we now begin to investigate whether a more realistic description supports this conclusion. The first possible source of error which comes to mind is the use of a sharp rapidity threshold, which in turn was based on a fictitious sharp cutoff in t. It is conceivable that a model with smooth t-damping would not exhibit the strong oscillations we have found; however, a simple argument shows that this is not the case. The essential point is that antibaryon production events occurring at rapidity intervals less than Δ_B (i.e., with large momentum transfer) are a small fraction of those reactions in which antibaryons are produced. Since antibaryons are only produced a fraction of the time, those events falling below the

rapidity threshold are a <u>very</u> small fraction of the total cross section, and their neglect should not lead to serious error. We can make these remarks quantitative:

Since we have shown that the presence of threshold-induced oscillations is correlated with the existence of complex poles in A(J), it is sufficient to show that the use of smooth damping does not introduce a major change in the position and residue of these poles. In our previous arguments we have taken the antibaryon kernel to be a delta-function in rapidity, as depicted in fig. 4.1a. We can introduce a smooth threshold by instead choosing a form like that of fig. 4.1b. There should of course be a smooth tail for $x > \Delta_B$, as in fig. 4.1c, but we shall treat this complication separately in the next section. Given a baryon kernel as in fig. 4.1b, it is straightforward to compute the Laplace transform and search for the poles of (3.13).. We have done this for a variety of choices for the function $G_B(x)$, all characterized by G_B being large only for x near Δ_B, and we find that the position and residue of the leading complex poles are only slightly altered. In ref. [11], an analysis based on the systematic use of a smooth t-dependence leads to similar oscillating effects. We conclude, then, that the oscillations do not depend in any essential way on an unrealistic t-dependence.

The preceeding discussion has treated baryon clusters in an inequitable manner by neglecting all other rapidity thresholds. This is not an unreasonable approximation, since the mass of a $B\bar{B}$ system is much larger than that of any other (known) meson cluster, but it is nevertheless instructive to attempt to include other cluster thresholds. Assuming that the propagator S is the same for all possible clusters (in other words, that the t-dependence is universal), and for simplicity that only one end-cluster is present, the only change in the above

formalism is to replace (3.11b) by

$$G(x) = \sum_M g_M \delta(x-\Delta_M) + g_B \delta(x-\Delta_B), \tag{4.1}$$

where the sum runs over the various possible meson cluster M, each with rapidity threshold Δ_M and integrated strength g_M. This leads to

$$A_{ab}(J) = \frac{g_a g_b e^{-(\Delta_a+\Delta_b)J}}{J-\beta-\sum_M g_M e^{-\Delta_M J} - g_B e^{-\Delta_B J}} .$$

With the semi-realistic formula (4.2) in hand we would like to compare the value of g_B required by the measured antibaryon cross section with the ABFST model estimate of section 2. In this case the quantity R_B of eq. (3.19), the slope of $\sigma_B(\eta)$ at threshold normalized to the total cross section there, is given by

$$R_B \approx \frac{g_B e^{-\Delta_B \alpha_0}}{1 + \sum_M \Delta_M g_M e^{-\Delta_M \alpha_0}} . \tag{4.3}$$

The additional factor is the derivative of the denominator of (4.2) evaluated at α_0, the position of the leading pole, and the equality is only approximate because there will be further complex poles arising from the meson threshold exponentials. In this case α_0 satisfies the equation

$$\alpha_0 - \beta - \sum_M g_M e^{-\Delta_M \alpha_0} = 0. \tag{4.4}$$

The facilitate the analysis, we suppose it is meaningful to speak of an average meson M-cluster threshold $\langle \Delta_M \rangle$ such that

$$\sum_M g_M \Delta_M e^{-\Delta_M \alpha_0} \equiv \langle \Delta_M \rangle \sum_M g_M e^{-\Delta_M \alpha_0}$$

$$\approx \langle \Delta_M \rangle e^{-\langle \Delta_M \rangle \alpha_0} \sum_M g_M . \tag{4.5}$$

From eq. (2.3), we suppose that this average meson-cluster threshold is related to the average squared-mass $\langle m_M^2 \rangle$ by

$$\langle \Delta_M \rangle = \Delta_B + \log \frac{\langle m_M^2 \rangle}{m_{B\bar{B}}^2} . \tag{4.6}$$

We can rearrange (4.3-5) into the ratio of baryon to meson cluster strengths:

$$\frac{g_B}{\sum_M g_M} \approx R_B e^{\alpha_0(\Delta_B - \langle \Delta_M \rangle)} \left(\langle \Delta_M \rangle + \frac{1}{\alpha_0 - \beta} \right) . \tag{4.7}$$

There is some numerical uncertainty in this result because of the freedom in the quantities entering on the right-hand side. We have tried the range of parameters

$$3 \le \Delta_B \le 5, \ -1 \le \beta \le 0, \ 0.6 \le \langle m_M^2 \rangle \le 1.2 \text{ GeV}^2,$$

together with $R_B \approx 0.3$, we find values of α_0 ranging from 0.75 to 0.85 and

$$2 \lesssim g_B / \sum_M g_M \lesssim 5.$$

The ABFST model estimates of the baryon kernel in section 2 suggest this ratio is at most 1. While these two estimates agree to order of magnitude, the size of the baryon kernel indicated by experiment is mysteriously large. However, given the crudeness and amount of extrapolation required for these estimates, we do not regard this as a critical discrepancy.

We can now give a sample calculation of a pp cross section based on these ideas. To specify the clusters involved we fall back on the pion-exchange model, and choose the ρ meson, a $K\bar{K}$ narrow resonance near threshold, and the aforementationed $B\bar{B}$ resonance. Inclusion of

the ρ is obvious, and a $K\bar{K}$ cluster is chosen because the $\pi\pi \to K\bar{K}$ integrated cross section [17] is of the same order of magnitude as that for $\pi\pi \to B\bar{B}$. We compute the various thresholds according to the rule (2.3), using a cutoff $T = 0.2\ \text{GeV}^2$. The end cluster is assumed to be always a Δ-resonance, and we compute its rapidity interval from (2.2b) with the same value of T. These choices lead to a $\bar{K}$-meson threshold of $s \approx 35\ \text{GeV}^2$, which roughly agrees with experiment [7]. To choose the coupling strengths, we note that the average multiplicity of cluster **i** is given by [12]

$$\langle n_i(\eta)\rangle = g_i \frac{\partial}{\partial g_i} \log A_{ab}(\eta),$$

and if the leading pole of the model is at $J = 1$, one has asymptotically

$$\langle n_i(\eta)\rangle \sim \text{constant} \times (g_i\, e^{-\Delta_i \eta}).$$

From the data on high-energy multiplicities [7] we choose the coupling strengths in the ratio

$$g_\rho e^{-\Delta_\rho} : g_K e^{-\Delta_K} : g_B e^{-\Delta_B} = 2:1:1\ .$$

These numbers are only meant to provide an illustration of threshold effects, and we do not claim they give a very accurate picture of cluster strengths. With this parametrization we obtain the cross section shown in fig. 4.2a. This result was obtained from the Regge expansion, where in this case three complex poles are needed for a reasonable approximation. For comparison, we show in fig. 4.2b the cross section that results if the K-meson cluster is omitted and the two remaining clusters are chosen with strengths in the ratio

$$g_\rho e^{-\Delta_\rho} : g_B e^{-\Delta_B} = 3:1,$$

and in fig. 4.3c we reproduce the result of section 3 with only the $B\bar{B}$ threshold retained.

There are two conclusions we wish to draw here. First, note that fig. 4.2a with two different neighboring meson thresholds shows less short-wavelength variation than fig. 4.2b, with only one. This indicates that nearby thresholds tend to interfere with each other or, in other words, their respective oscillations tend to be out of phase and cancel. Secondly, the oscillations associated with the $B\bar{B}$ resonance are not significantly altered by meson thresholds. The essential ingredient here is the fact that the mass of a $B\bar{B}$ system, and thus its associated rapidity threshold, is significantly above that of the other important clusters in the multiperipheral chain.

This discussion has, of course, oversimplified matters by attributing meson production to two or three isolated zero-width resonances, and one might wonder what happens if the cluster spectrum approaches a continuum. We have investigated this point by calculating the cross section resulting from various other choices of kernel characterized by G(x) being a continuous function with a prominent peak at $x = \Delta_B$. The conclusions of the previous paragraph are upheld, and we find cross sections that resemble the simple model of section 3. However, many complex poles are needed to provide a good approximation to the exact cross section.

As a byproduct of this analysis, it is possible to discuss other reactions along the same lines. If we consider the even-signature πp total cross section,* the sum of $\pi^+ p$ and $\pi^- p$, the only change is that a pion must be coupled to one end of the multiperipheral chain. There are now three possibilities, depending on whether the end cluster is a ρ, $K\bar{K}$, or $B\bar{B}$ system. In the numerator of eq. (4.2) we replace one factor of

*The Kp system is complicated by the presence of several non-leading Regge trajectories.

$g_p e^{-\Delta_p J}$ by $g_\rho e^{-\tilde{\Delta}_\rho J} + g_K e^{-\tilde{\Delta}_K J} + g_B e^{-\tilde{\Delta}_B J}$, where the g_i are the same but $\tilde{\Delta}_i$ differs from Δ_i because the threshold kinematics at the end of the multiperipheral chain differs from that of its interior. Using eqs. (2.2) with the same cutoff $T = 0.2\ \text{GeV}^2$, we obtain fig. 4.3. In this case, because the various clusters can be produced at the ends as well as in the middle of the chain, the baryon threshold is not isolated. Its consequent oscillation is reduced considerably, and is susceptible to being washed out by the threshold effects of other clusters. We have only included two possible clusters, so in a more realistic model this smoothing is likely to be even more pronounced than that which appears in the figure. If we ignore this caveat, the model predicts an increase of up to 2 mb in the sum of $\pi^- p$ and $\pi^+ p$ cross sections from Serpukhov to ISR energies.

This would have been a good apportunity to discuss inclusive cross sections; unfortunately, the model we have been using is somewhat inappropriate. The reason is that an inclusive cross section in a multiperipheral model depends critically on the details of momentum transfer damping and cluster decay which we have very crudely approximated. In fig. 2.4, for example, the antibaryon inclusive spectrum will be quite sensitive to the t-dependence of the pion links as well as the characteristics of the $B\bar{B}$ system, and our averaging procedure will not be reliable.

5. INCLUSION OF BARYON EXCHANGE

In the preceding discussion the baryon-antibaryon system has been treated as a single narrow resonance, and we now attempt to improve the description by allowing it a high-energy component due to baryon exchange (fig. 3.6). This will not alter the general characteristics of the

threshold effects and oscillations, as we shall see, but does lead to an intriguing interpretation of the earlier results and suggests that the complex poles we have found may be identified with the P' Regge singularity. The arguments to follow will be based on a model formally identical to that of ref. [21], but differing in interpretation.

Consider an idealized situation in which there is one species of self-conjugate meson (M), one species of baryon (B) together with the corresponding antibaryon ($\bar{B}$), and where at first the meson system does not couple to the baryons. The forward absorptive part of the meson scattering amplitude, in the multiperipheral approximation, then has the form shown in fig. 5.1, where we assume some meson cluster is emitted at each vertex with strength γ_M and the sides of the "ladder" correspond to the exchange of a single effective Regge trajectory α_M. Similarly, baryon scattering is as shown in fig. 5.2, where again a meson cluster (not necessarily the same as in MM scattering) is emitted at each vertex with strength γ_B and there is an effective (baryon) Regge exchange α_B. Since only mesons are emitted, threshold factors are omitted. At this stage, because of the decoupling assumption, BB scattering does not occur. We must be more explicit about the signature of the baryon system: the model just described should be specified separately for even and odd signature ($BB \pm \bar{B}\bar{B}$ in the s-channel or $B\bar{B} \pm \bar{B}B$ in the t-channel). At present, however the model is so simple that both signatured amplitudes are equal and we have an exactly exchange degenerate situation. (From this point of view, the BB scattering amplitude vanishes because it is the difference of the even and odd signatured amplitudes.) To identify the Regge singularities involved, we "sum the ladders" to find the respective

forward absorptive parts:*

$$A_M(J) \propto \Sigma \frac{1}{J-\alpha_M} \gamma_M \frac{1}{J-\alpha_M} \gamma_M \cdots \gamma_M \frac{1}{J-\alpha_M}$$

$$= \frac{1}{J-\alpha_M-\gamma_M},$$

and similarly

$$A_B^{(\pm)}(J) \propto \frac{1}{J-\alpha_B-\gamma_B}.$$

If we assume that meson exchange producing meson clusters accounts for the bulk of multiparticle events, then the singularity of A_M should not differ drastically from the Pomeron, and its intercept should not lie too far from one. We suppose

$$\alpha_M + \gamma_M \equiv \alpha_0 \approx 0.9$$

where this value will be justified below. $A_B^{(\pm)}$, on the other hand, corresponds to $B\bar{B}$ annihilation to mesons; in the $p\bar{p}$ case this is approximately equal to the difference between pp and $p\bar{p}$ total cross sections, usually attributed to the ω Regge trajectory [22]. Hence we assume

$$\alpha_B + \gamma_B \equiv \alpha_\omega \approx 0.5. \tag{5.2}$$

At this stage we have exchange degenerate ω and P' poles in $A_B^{(-)}$ and $A_B^{(+)}$.

Now we couple the even-signatured meson and baryon systems by introducing a vertex for (exchanged meson) + (exchanged baryon) → (produced baryon). We write the associated coupling as $\left(g_B e^{-\Delta J}\right)^{1/2}$, since the product of two of these corresponds to the old vertex for $\pi\pi \to B\bar{B}$. The exponential factor will provide the proper energy

*Note: MM scattering is purely even signature.

threshold for production of a $B\bar{B}$ pair. The various vertices now present in the model are shown in fig. 5.3. Because of the coupling between channels, the poles at α_0 and α_ω will mix to form two new singularities in the even-signature amplitude, and P'-ω exchange degeneracy will be broken.

The coupled system is most easily handled in a matrix formalism, and a simple equation is obtained if we factor off the ends of the multiperipheral chain, analogously to our procedure in section 3. There are then two channels, associated with meson and baryon exchange, and the forward amplitudes satisfy the canonical multiperipheral equation

$$A = G + GSA \tag{5.3}$$

depicted in fig. 5.4, where

$$A = \begin{pmatrix} A_{MM} & A_{MB} \\ A_{MB} & A_{BB} \end{pmatrix}, \tag{5.4a}$$

$$S = \begin{pmatrix} (J-\alpha_M)^{-1} & 0 \\ 0 & (J-\alpha_B)^{-1} \end{pmatrix}, \tag{5.4b}$$

$$G = \begin{pmatrix} \gamma_M & \left(g_B e^{-\Delta_B J}\right)^{1/2} \\ \left(g_B e^{-\Delta_B J}\right)^{1/2} & \gamma_B \end{pmatrix} \tag{5.4c}$$

and the (+) signature label has been suppressed. If eq. (5.3) is solved for A, the J-singularities consist of poles whose location is given by the vanishing of a denomination function

$$\begin{aligned} D(J) &\equiv (J-\alpha_M)(J-\alpha_B) \det(1-GS) \\ &= (J-\alpha_0)(J-\alpha_\omega) - g_B e^{-\Delta_B J}. \end{aligned} \tag{5.5}$$

In fig. 5.5 we separately plot the quadratic (solid line) and exponential (dashed line) terms in D, for small (unrealistic!) values of g_B. The zeros of D at α_0 and α_ω in the uncoupled case have been shifted apart slightly, and in addition a third zero appears in the left half-plane. For slightly larger g_B, the exponential in effect shifts to the right, so the two leading zeros are further split apart, while the third moves to the right. As g_B increases further, the two non-leading zeros collide and move off into the complex plane: see fig. 5.6. At the experimentally-relevant values of g_B (and Δ_B) the situation is as indicated in fig. 5.6: a leading real pole (α_P - the Pomeron) plus a complex conjugate pair (α_c). In addition there will be a family of lower-lying complex poles, like those appearing in fig. 3.2, which are negligible once moderate energies are reached.

We are now in a position to argue that the leading complex pole, α_c, should be identified with the P' Regge trajectory. Suppose we expand A(J) in powers of the antibaryon coupling,

$$A(J) = \frac{a(J)}{(J-\alpha_0)(J-\alpha_\omega)} + \sum_{n=1}^{\infty} \left[g_B e^{-\Delta_B J} \right]^n b_n(J), \qquad (5.6)$$

[a(J) and $b_n(J)$ are matrices] and consider the inverse Laplace transform (3.15). For energies below the antibaryon threshold, all terms in the integrand containing one or more powers of $e^{-\Delta_B J}$ decrease exponentially as $\mathrm{Re}J \to +\infty$, and if the contour is closed to the right they do not contribute. Therefore, in this energy range only, the amplitude is in effect given by the first term of (5.6) and can be represented by the two poles at α_0 and α_ω. The latter is the even-signature exchange degenerate partner of the ω trajectory which should clearly be identified with the P'. However, it is not obligatory to expand A(J) as in (5.6);

and one can equally well work with the singularities of the full amplitude—the poles α_P and α_c associated with the full denominator function (5.5). Below the antibaryon threshold either set of singularities must give the same cross section (to the extent that the lower-lying complex poles may be neglected). It has been shown in the previous paragraph that, in the presence of the antibaryon coupling, α_ω "turns into" α_c, and α_c is therefore the approximately exchange-degenerate partner of the ω trajectory. The overall situation is as follows: Below the antibaryon threshold one can work with a "bare" Pomeron $\alpha_0 \approx 0.9$ and exactly exchange-degenerate ω-P' trajectories or with a renormalized Pomeron $\alpha_P = 1.0$, a complex pair α_c, and a real ω. Above the antibaryon threshold, however, one must use the second set of singularities, and breaking of P'-ω exchange degeneracy relationships should appear.

To discuss cross sections in this model it is necessary to couple external particles to the multiperipheral chain, and at this point a technical difficulty arises. For BB scattering, say, the model should include processes such as in fig. 5.7 in which an external baryon couples to a baryon trajectory. The kinematics, unfortunately, are such that a baryon-exchange link coupled to an external baryon can involve positive momentum transfers, and in this case the foregoing analysis—based on strictly spacelike t—is inapplicable. Furthermore, since the average baryon momentum transfers for such exchanges will certainly differ from the corresponding quantity for "internal" baryon exchange, at the least some new parameters will be required, and a decent treatment would require a specific choice of t-dependence. This is more detail than we care to go into, and we shall make the approximation of neglecting such effects. No particular threshold mechanism is involved in

such processes, and their neglect should not affect our conclusions.* In particular, the Regge pole spectrum is independent of this approximation since it does not depend on "external" couplings.

We now consider the immediately interesting case of (even-signature) pp scattering and suppose as before that the leading clusters are always either a nucleon or Δ-resonance. The elastic amplitude is then as shown in fig. 5.8, and given by

$$A_{pp}^{(+)}(J) = g_p\, e^{-\Delta_p J}\left[\frac{1}{J-\alpha_M} + \frac{1}{J-\alpha_M}\, A_{MM}(J)\, \frac{1}{J-\alpha_M}\right] g_p\, e^{-\Delta_p J}, \quad (5.7)$$

and evaluating this expression from eqs. (5.3-5) we find

$$A_{pp}(J) = \left[g_p\, e^{-\Delta_p J}\right]^2 \frac{J-\alpha_\omega}{D(J)} . \quad (5.8)$$

If the antibaryon term in D(J) is neglected, for energies below its threshold, then this formula reduces (as it must) to an expression proportional to $(J-\alpha_0)^{-1}$.

The parameters entering into (5.8) can be estimated in a manner by now familiar. We choose $\alpha_\omega = 0.5$ as stated and the same thresholds as previously. The BB coupling g_B and the "bare Pomeron" intercept α_0 are constrained by the two requirements of reproducing fig. 1 and generating a leading pole at J = 1. This leads to values of g_B similar to those obtained previously and α_0 near 0.9. Not surprisingly, the model gives the same quality of agreement with experiment as its predecessors.

*Processes like that of fig. 5.7 are of interest, for example, when studying the inclusive leading proton spectrum for $x \neq 1$; see ref. [23].

In this case, however, the leading complex pole position is typically around $0.5 \pm 0.5\, i$—the imaginary part has been roughly halved and the consequent period of oscillation doubled to approximately 12 units of rapidity. The reason, of course, is that by allowing a high-energy component to the $B\bar{B}$ system we have increased its effective mass and, from eq. (2.3), have thereby effectively increased its rapidity threshold. Unfortunately, this reduces the likelihood of foreseeable experiments observing a full oscillation, rather than a simple increase, in the total cross section.

6. DIFFRACTIVE EFFECTS

The models previously discussed in this paper may be described as referring to the short-range correlation component [24] of high-energy scattering, in that (exclusive) Pomeron-exchange amplitudes have not been considered. In other words, we have omitted the "high-energy tail" of the multiperipheral kernel. While it is not our aim in this paper to provide a complete discussion of diffraction scattering, it is necessary to show that its inclusion does not alter the general features of the threshold and oscillatory effects we propose. Specifically, Pomeron exchange will be introduced here in a manner based on the "schizophrenic Pomeron" model of Chew and Snider [25]. We will find that the oscillatory behavior is essentially unchanged, and it will be evident from the discussion that the conclusion is somewhat insensitive to the precise way in which diffraction is introduced. (Further remarks on this point are in the next section.)

In parametrizing the high-energy tail we can take advantage of two useful facts. First, since the most-favored configuration in a multiperipheral model is a roughly uniform distribution in rapidity, the observed mean multiplicity tells us that the probability of a large

subenergy will be small unless the total energy is enormous. The extremities of the high-energy tail in the kernel, then, will not contribute greatly at accessible energies, and it is natural to replace its probably complicated J-plane structure by a simpler approximation. Secondly, we use the phenomenological observation that the high-energy tails of scattering amplitudes approximately factorize with respect to the incident particles,* and this fact suggests that as a first approximation we treat the tail as a simple pole.** For the moment, we will take the pole intercept as a free parameter, and in the appendix we will return to discuss its origins and the possibility of improving the approximation.

We consider a multiperipheral model based on exchange of a single effective meson trajectory (M) and whose kernel contains a narrow-resonance meson cluster at low subenergy, a $B\bar{B}$ resonance localized near threshold, and a high-energy tail in the MM scattering amplitude due to (interfering) P and P' exchange. The components of the kernel are shown in fig. 6.1, and we write the corresponding vertices as g_M, $g_B e^{-\Delta_B J}$, and $\epsilon^2 S_P(J)$. In the latter quantity, ϵ represents the coupling of M to (P + P') and, with our approximations, the Pomeron propagator is

$$S_P(J) = \frac{1}{J-\alpha_c} , \qquad (6.1)$$

where α_c is now the position of the single effective pole. Since the kernel is much larger in the resonance region than its high energy tail, we expect g_M and g_B to be much larger than ϵ. More explicitly, g_M and g_B should not change drastically from their previous values, of order

*In particular, the residues of the Pomeron and P' are proportional [26].

**This idea has had considerable recent popularity in both phenomenological [27] and theoretical [28] applications.

one, while in the Appendix we estimate $\epsilon \approx 0.01$-0.1.

We write the meson exchange Regge propagator as

$$S_M(J) = \frac{1}{J-\beta_M} , \qquad (6.2)$$

where β_M is to be understood as $2\bar{\alpha}_M - 1$, $\bar{\alpha}_M$ being an average meson spin. To complete the specification of the model we assume the external particles are attached as before: external protons couple through either a nucleon or Δ-resonance via either meson or Pomeron exchange, as shown in fig. 6.2. The amplitude may now be written succinctly in a two-channel matrix formalism, where now the channels refer to M and (P+P'):

$$A_{pp}(J) = B_p^T(J)[S(J) + S(J)\,A(J)\,S(J)]B_p(J), \qquad (6.3)$$

where the external coupling vector is

$$B_p(J) = \begin{pmatrix} r_M e^{-\Delta_p J} \\ r_P \end{pmatrix} , \qquad (6.4)$$

the propagator matrix is

$$S(J) = \begin{pmatrix} S_M(J) & 0 \\ 0 & S_P(J) \end{pmatrix} , \qquad (6.5)$$

and A(J) satisfies the equation

$$A(J) = G(J) + G(J)\,S(J)\,A(J) , \qquad (6.6)$$

where now the kernel matrix is

$$G(J) = \begin{pmatrix} g_M + g_B e^{-\Delta_B J} & \epsilon \\ \epsilon & 0 \end{pmatrix} . \qquad (6.7)$$

The M-M element of G represents the resonant part of the kernel, the

sum of the first two terms in fig. 6.1, while the M-P coupling is the Regge residue ϵ and the P-P element is assumed to be negligible. Solving this system of equations we find

$$A_{pp}(J) = B_p^T(J)\, \tilde{A}(J)\, B_p(J)\,, \tag{6.8}$$

where

$$\tilde{A}(J) = \frac{1}{D(J)} \begin{pmatrix} 1 & \dfrac{\epsilon^2}{J-\alpha_c} \\ \dfrac{\epsilon^2}{J-\alpha_c} & \dfrac{J-\alpha_0-g_B e^{-\Delta_B J}}{J-\alpha_c} \end{pmatrix}. \tag{6.9}$$

We have defined $\alpha_0 \equiv g_M + \beta_M$, and the denominator function is

$$D(J) = J-\alpha_0 - g_B e^{-\Delta_B J} - \frac{\epsilon^2}{J-\alpha_c}\,. \tag{6.10}$$

In discussing this result, it is convenient to consider various special cases. If $\epsilon = 0$ (no exclusive Pomerons) and $g_B = 0$ (no antibaryon production) we have

$$\tilde{A}(J) = \begin{pmatrix} \dfrac{1}{J-\alpha_0} & 0 \\ 0 & \dfrac{1}{J-\alpha_c} \end{pmatrix},$$

which yields*

$$\sigma_{pp}(\eta) = r_M^2\, e^{(\alpha_0-1)\eta} + r_P^2\, e^{(\alpha_c-1)\eta} \qquad (\epsilon = g_B = 0). \tag{6.11}$$

*The thresholds associated with the ends of the chain are not essential to this discussion, so in the remainder of this section we set $\Delta_p = 0$ to simplify the notation.

The first term is the inelastic cross section, which has been built up by the repetition of meson clusters, and the second is the elastic cross section, given by the aforementioned average of P and P' exchanges. Next, if $\epsilon = 0$ but $g_B \neq 0$, it is easy to see that the inelastic cross section is identical to the simple antibaryon model of section 3. The elastic scattering term is unchanged; in fact, even in the general case of ϵ and $g_B \neq 0$ elastic scattering is still given by the second term in the lost equation. This crude, single-pole approximation will deteriorate in accuracy for higher energies.

The case $\epsilon \neq 0$ but $g_B = 0$ is the original schizophrenic Pomeron model; there are now two poles, given by the vanishing of

$$D(J) = J-\alpha_0 - \frac{\epsilon^2}{J-\alpha_c} \qquad (g_B = 0)$$

and located at

$$\alpha_\pm = \tfrac{1}{2}(\alpha_0+\alpha_c) \pm \sqrt{\tfrac{1}{4}(\alpha_0-\alpha_c)^2 + \epsilon^2}\,.$$

For smal ϵ^2, the experimentally relevant situation, this becomes $\alpha_+ \approx \alpha_0 + \delta\alpha$, $\alpha_- \approx \alpha_c - \delta\alpha$, where $\delta\alpha = \epsilon^2(\alpha_0-\alpha_c)^{-1}$. The (even-signature) total cross section is now

$$\sigma_{pp}(\eta) = r_+ e^{(\alpha_+-1)\eta} + r_- e^{(\alpha_--1)\eta} \qquad (g_B = 0) \tag{6.13}$$

where

$$r_\pm = \frac{1}{D'(\alpha_\pm)}\left[r_M^2 + \frac{2r_M r_P \epsilon^2 + r_P^2(\alpha_\pm - \alpha_0)}{\alpha_\pm - \alpha_c}\right]. \tag{6.14}$$

In view of our earlier remarks we expect that until η is large the contribution of exclusive Pomeron exchange should be small and (6.13) should be approximately equivalent to (6.11). Indeed, it can be shown

directly that (6.13) differs from (6.11) only by terms of order $\epsilon^2\eta$, and for small values of the latter quantity one can describe the inelastic cross section adequately by α_0 above. A higher energies α_+ will dominate, and since $\alpha_+ > \alpha_0$ the cross section will fall (slightly) less rapidly than in the absense of diffractive effects. Another way to see this is to note that the extra terms in ϵ are positive definite. A similar result will hold for the dependence of a scattering amplitude on any subenergy.

Returning to our major concern after this disgression, we now consider a non-vanishing antibaryon coupling. Below the antibaryon threshold the cross section is identical to that of the schizophrenic Pomeron model just described. Above the threshold antibaryons appear, and it is almost self-evident that the situation is roughly the same as in the simpler model of section 3. The only difference, after all, is that the other parts of the multiperipheral chain have been made more complicated in that a combination of two Regge poles is used in their description, leading to a gentler energy dependence, and an elastic scattering term has been added. To be explicit, if we use the same values of g_B and Δ_B as before, determine ϵ from triple Regge couplings (see the Appendix) and α_c from the pp elastic cross section (at energies below the antibaryon threshold), and constrain α_0 so as to produce a leading pole at $J = 1$, we find a cross section greatly resembling that obtained with diffraction omitted (fig. 3.4) with roughly the same set of complex poles. The essential reason that the inclusion of exclusive Pomeron effects has not altered our conclusions is that at presently accessible energies these complications are a small effect, whereas antibaryon production is a large effect.

7. CONCLUDING REMARKS

We have shown in this paper that the essential features of the threshold and rising effects in the antibaryon and pp total cross sections can be nicely correlated and understood within simple multiperipheral models. With the possible exception of the size of the antibaryon kernel, such models successfully account for the thresholds, energy dependence, and increase in magnitude of both cross sections. We were then led to a simple description in terms of complex Regge poles and the prediction of asymptotic oscillations in cross sections.

A crucial question which immediately arises is whether the oscillatory behavior is an artifact of the model used. We have investigated this by attempting to make the model realistic in several different ways—by including other thresholds, a better antibaryon kernel, and diffractive effects—and found no essential change. Another potential source of criticism is our use of a sharp cutoff in momentum transfer, but we have argued that this is not an essential requirement. There remain, however, other possible means of avoiding asymptotic oscillations which we have not mentioned:

1. The existence of an indefinite sequence of other important particle-clusters of increasing mass. In this case, new thresholds might be reached before the antibaryon-induced oscillations can manifest themselves. While there is no evidence for the existence of such new clusters, we cannot rule out their existence.

2. The antibaryon kernel may be so large that the naive summation of kernels in eq. (4.2) generates a leading pole above $J = 1$, and eventually unitarity effects restore the Froissart bound.* In this case the

*Suzuki [5] discussed the connection between antibaryon production and the pp total cross section in this manner.

cross section may increase approximately as a power of s temporarily, and eventually as $(\log s)^2$, with no oscillation.

3. Unitarity effects related to the Pomeron might invalidate the simple model used here. While this is possible, the unitarity bounds on the pp amplitude are in no danger of saturation [1], and there is no reason to believe that such effects are large enough to affect the gross behavior of the cross section at foreseeable energies.

4. It has been claimed [19] that unitarity effects within the coupled $B\bar{B}$-many pion system invalidate simple multiperipheral arguments. We disagree with this assertion; in the pion-exchange case it is known from the success of Chew-Low extrapolations that any such effects must be of short range in rapidity, and thus the resonance description of the coupled system in section 2 should suffice.

The best test of the ideas presented here would, of course, be the observation of a genuine oscillation. Unfortunately, our estimates of the period very likely rule this out for the present. For inclusive cross sections the amplitude of oscillation is likely to be much larger, but on the other hand the period doubles [8]. The most accessible test, it seems, is based on the fact that the oscillation in the ratio of real to imaginary part of the elastic amplitude is advanced by one-quarter cycle over the total cross section, and this quantity would pass through its maximum at lower energy.

In this paper we have not touched upon the t-dependence of the amplitude. The main reason for this is simplicity—the sharp cutoff approximation which makes the models discussed here so tractable is obviously inadequate if one wishes to study the variation in t. Furthermore such a discussion would require considerably more input of information on choice of propagator, off-shell effects, and so on, and we

have tried to use as few parameters as possible. This subject certainty deserves further study.

A very interesting question we have only touched on is the relation of the complex poles to the conventional set of non-leading Regge singularities. In the model of section 5, involving a baryon exchange component in the kernel, the complex pole is naturally identified with the P', while in the model of section 6, where diffraction has been combined with a narrow resonance $B\bar{B}$ kernel, one finds the P' and complex poles appearing as distinct singularities. If the two models are simply combined, by including both effects in the kernel, there would still be two distinct singularities. Aside from the point of principle, this is a matter of considerable phenomenological interest, since its answer would dictate the number of distinct Regge poles to be used in fitting data. Unfortunately, the present arguments do not provide a resolution to this question.*

ACKNOWLEDGMENT

It is a great pleasure to thank Geoffrey Chew for his extensive assistance and encouragement in all phases of this work. Discussions with a number of people, particularly Thomas Neff and Mahiko Suzuki, have been of much assistance.

*After the manuscript was completed we received a preprint by Tan [29] which provides further discussion of some of the topics considered in this paper.

APPENDIX

The description of the schizophrenic Pomeron model used to incorporate diffraction in section 6 was rather brief, and we wish to present a more detailed discussion which emphasizes the physical approximations involved. The analysis is most understandable if we imagine a set of different regimes of total energy.

I. $\eta \approx 0\text{-}2$:* the inelastic cross section will be dominated by the production of only a small number of meson clusters. Pomeron exchange amplitudes are possible, but since the various subenergies cannot be large, their contribution may be neglected.** The energy dependence of the inelastic cross section is

$$\sigma_{\text{inel}}(\eta) \propto e^{(\beta_M - 1)\eta}(1 + \gamma_M \eta + \cdots).$$

II. $\eta \approx 2\text{-}4$: multiple production of meson clusters occurs, while the total energy is still too low for exclusive Pomeron exchange to be important. The energy dependence is

$$\sigma_{\text{inel}}(\eta) \propto e^{(\beta_M - 1)\eta} \sum_n (\gamma_M \eta)^n / n!$$

$$= e^{(\gamma_M + \beta_M - 1)\eta} = e^{(\alpha_0 - 1)\eta},$$

and the bare Pomeron provides a reasonable description of the inelastic cross section.

---

*Recall $s = 2m_p^2(1 + \cosh \eta)$.

**The dependence on rapidity interval y of the meson propagator is $\gamma_M^2 e^{\beta_M y}$, compared to $\epsilon^2 e^{\alpha_c y}$ for the Pomeron propagator. Since γ_M is much larger than ϵ and α_c is 0.5-1.5 units above β_M, Pomeron exchange only becomes an important ingredient once large y is possible.

III. $\eta \gtrsim 4$: the incident energy is now sufficiently high that exclusive Pomeron exchange becomes important. If we consider eqs. (6.8-10) for the amplitude, this means we cannot neglect terms in ϵ and the relevant Regge singularities are the two poles $\alpha_\pm$ of (6.12). The presence of a diffractive tail has thus "split" the bare Pomeron α_0 into two poles α_+ and α_-, to be identified with the P and P' respectively, which should provide a simple parametrization of σ_{inel} for large η. For lower values of η, in energy regime II for example, we can still use α_+ and α_-, but it is more economical and physically equivalent to use just α_0. This is because α_0 "differs" from the combination of α_+ and α_- just by processes which are negligible in region II. However, in region III α_0 is inadequate and $\alpha_\pm$ must be used.

One can iterate this procedure by successively improving the description of the exclusive Pomeron amplitude (see also ref. [28]). Since the singularity at α_c represents the elastic cross section, over a range of energies where the elastic amplitude is proportional to $e^{\alpha(t)\eta}$, one should interpret α_c as $2\alpha(\langle t \rangle) - 1$. When we introduce an internal Pomeron component in region III, since the typical internal subenergies are much lower, say in region II, the appropriate choice is $\alpha_c \approx 2\alpha_0 - 1$ (neglecting the effect of trajectory slope). If we were to introduce a region IV, for example $\eta \approx 7\text{-}10$, the typical internal subenergies would be unlikely to exceed those of region III and α_c should be understood as the three poles $2\alpha_+ - 1$, $\alpha_+ + \alpha_- - 1$, and $2\alpha_- - 1$. One could then include all three in the multiperipheral equation to give the elastic amplitude appropriate for this region, which would involve four Regge poles. One could also introduce this complicated Regge spectrum in the lower-energy region III, but the resulting description would only be an inefficient and physically equivalent alternative to $\alpha_\pm$ (just as $\alpha_\pm$ are an

inefficient alternative to α_0 in region II). This procedure can be repeated indefinitely, at the cost of complicating the description as the incident energy increases. The result would be a sequence of energy regimes such that in region N one determines the elastic amplitude by parametrizing the exclusive Pomeron amplitudes in the manner appropriate to region N-1. The description appropriate for region N is valid although unnecessarily complicated in regions $1, 2, \cdots, N-1$, and inadequate for regions $N+1$, $N+2$, $\cdots$.

One might wonder what happens to the threshold effects under this iterative procedure. It turns out that the position and residue of the leading complex pole is stable under (at least) the first step of the iteration. The reason is essentially that this complex pole is "responsible" for generating the antibaryon thresholds in the asymptotic expansion, and should not be significantly altered by the inclusion of Pomeron fine structure.

Finally, we turn to the estimation of ϵ. Consider double diffraction dissociation into (moderately) large masses, shown in fig. A.1a. To lowest order in the small parameter ϵ, the contribution of this process to the forward elastic amplitude is shown in fig. A.1b, and from the formulae in section 6 it is given by

$$r_M \; \frac{1}{J-\alpha_0} \; \epsilon \; \frac{1}{J-\alpha_c} \; \epsilon \; \frac{1}{J-\alpha_0} \; r_M \, .$$

On the other hand, in a model with a single (moving) Regge trajectory $\alpha_0(t)$ with residue function $r(t)$ and triple-Regge coupling $g(t)$, and conventional normalization, the expression corresponding to this figure is [28]

$$r(0) \; \frac{1}{J-\alpha_0(0)} \cdot \int_{-\infty}^{0} \frac{dt}{16\pi} \; \frac{g^2(t)}{J-2\alpha_0(t)+1} \cdot \frac{1}{J-\alpha_0(0)} \; r(0).$$

As we have said, it is a reasonable approximation at moderate energies to take

$$\alpha_c \approx 2\alpha_0(\langle t \rangle) - 1,$$

and comparing the two expressions we identify

$$\epsilon^2 \approx \frac{1}{16\pi} \int_{-\infty}^{0} dt \; g^2(t) \, .$$

If several trajectories are present, ϵ^2 is an average of such terms. Using triple-Regge couplings obtained either from a single bare-Pomeron parametrization [27] or more conventional fits [2], together with $g(t)$ having a width in t of 1-2 GeV^{-2}, we find typical values

$$\epsilon^2 \sim 0.01 - 0.1.$$

REFERENCES

[1] U. Amaldi, Proceedings of the 1973 Aix-en-Provence Conference on Elementary Particles, J. Physique 34 (1973), Supplement No. 10, C241.

[2] L. Foà, ibid., C317.

[3] J. C. Botke, Nucl. Phys. B51 (1973) 586.
L. Caneschi, Nucl. Phys. B68 (1974) 77.
R. Blutner, Karl Marx Univ. preprint KMU-HEP-7311 (1973).

[4] D. Sivers and F. von Hippel, Phys. Rev. D 9 (1974) 830.

[5] M. Suzuki, Nucl. Phys. B64 (1973) 586.

[6] T. K. Gaisser and C. -I Tan, Phys. Rev. D 8 (1973) 3881.

[7] M. Antinucci et al., Lett. al Nuovo Cimento 8 (1973) 121.

[8] G. F. Chew and J. Koplik, Phys. Lett. 48B (1973) 221.

[9] G. F. Chew and D. R. Snider, Phys. Lett. 31B (1970) 75;
M. L. Goldberger, D. Silverman, and C.-I Tan, Phys. Rev. Lett. 26 (1971) 100.

[10] C. Quigg, in Particles and Fields - 1973, Proceedings of the Berkeley Meeting of the APS/DPF (American Physical Society, 1973);
E. Berger, CERN preprint TH. 1700 (1973).

[11] G. F. Chew and J. Koplik, Peripheral Thresholds and Regge Asymptotic Behavior, LBL-3014 (1974).

[12] L. Bertocchi, S. Fubini and M. Tonin, Nuovo Cimento 25 (1962) 626;
D. Amati, S. Fubini and A. Stanghellini, ibid., 26 (1962) 896.

[13] G. F. Chew, T. Rogers, and D. R. Snider, Phys. Rev. D 2 (1970) 765.

[14] N. F. Bali, G. F. Chew, and A. Pignotti, Phys. Rev. 163 (1967) 1572.

[15] G. Grayer et al., Phys. Lett. 39B (1972) 563.

[16] Particle Data Group, UCRL-20000NN (1970), LBL-58 (1972).

[17] S. D. Protopopescu et al., Phys. Rev. D 7 (1973) 1279.

[18] J. S. Ball and G. F. Chew, Phys. Rev. 109 (1957) 1385;
R. J. N. Phillips, Rev. Mod. Phys. 39 (1967) 681.

[19] M. B. Einhorn and S. Nussinov, NAL-Pub-73/79-THY.

[20] C. F. DeTar, Phys. Rev. D 3 (1971) 128.

[21] J. Koplik, Phys. Rev. D 7 (1973) 3317.

[22] H. Goldberg, Phys. Rev. D 6 (1972) 2542.

[23] L. Caneschi and A. Pignotti, Phys. Rev. Lett. 22 (1969) 1219.

[24] H. Harari, Weizmann Institute Preprint WIS/73/32 Ph (1973 Scottish Universities Summer School Lectures), and refs. therein.

[25] G. F. Chew and D. R. Snider, Phys. Rev. D 1 (1970) 3453, ibid. D 3 (1971) 420.

[26] R. Carlitz, M. B. Green, and A. Zee, Phys. Rev. D 4 (1971) 3439.

[27] J. Dash, Phys. Rev. D 9 (1974) 200.
N. F. Bali and J. Dash, Argonne preprints ANL/HEP 7372 (1973), 7370 (1974).

[28] W. R. Frazer, D. R. Snider, and C. -I. Tan, Phys. Rev. D 8 (1973) 3180; D. Amati, L. Caneschi and M. Ciafaloni, Nucl. Phys. B62 (1973) 173; J. Finkelstein, Phys. Rev. D 8 (1973) 4176;
M. Bishari, G. F. Chew, and J. Koplik, Nucl. Phys. B72 (1974) 61, 93.

[29] C. -I Tan, Brown University preprint COO-3130TA-305 (1974).

FIGURE CAPTIONS

Fig. 1. Integrated antibaryon inclusive cross section as a function of energy.

Fig. 2.1. Production of N + 2 clusters of particles in the ABFST model.

Fig. 2.2. Possible antibaryon-producing clusters.

Fig. 2.3. Experimental $\pi^+\pi^- \to p\bar{p}$ cross section.

Fig. 2.4. Amplitude controlling the antibaryon threshold.

Fig. 3.1. One-dimensional multiperipheral model.

Fig. 3.2. Regge-pole spectrum of eq. (3.13).

Fig. 3.3. Cross sections resulting from (3.13): exact (solid line), three-pole asymptotic expansion (dashed line), and partial (dotted lines).

Fig. 3.4. Even-signatured pp total cross section compared to "experiment."

Fig. 3.5. Ratio of real to imaginary parts of the forward scattering amplitude.

Fig. 3.6. Large-mass component of the $B\bar{B}$ system.

Fig. 4.1. Possible antibaryon kernels.

Fig. 4.2. Total cross section with (a) ρ, $K\bar{K}$, and $B\bar{B}$ thresholds, (b) ρ and BB thresholds, and (c) $B\bar{B}$ threshold only.

Fig. 4.3. Even-signatured πp total cross section.

Fig. 5.1. Uncoupled meson system.

Fig. 5.2. Uncoupled baryon system.

Fig. 5.3. Vertices in the coupled meson-baryon system.

Fig. 5.4. Multiperipheral equation.

Fig. 5.5. Quadratic (solid line) and exponential (dashed line) factors in eq. (5.5).

Fig. 5.6. Motion of Regge poles as a function of g_B.

Fig. 5.7. A contribution to BB scattering.

Fig. 6.1. Components of the kernel in the (extended) schizophrenic Pomeron model.

Fig. 6.2. End vertices.

Fig. A.1. Double diffraction dissociation.

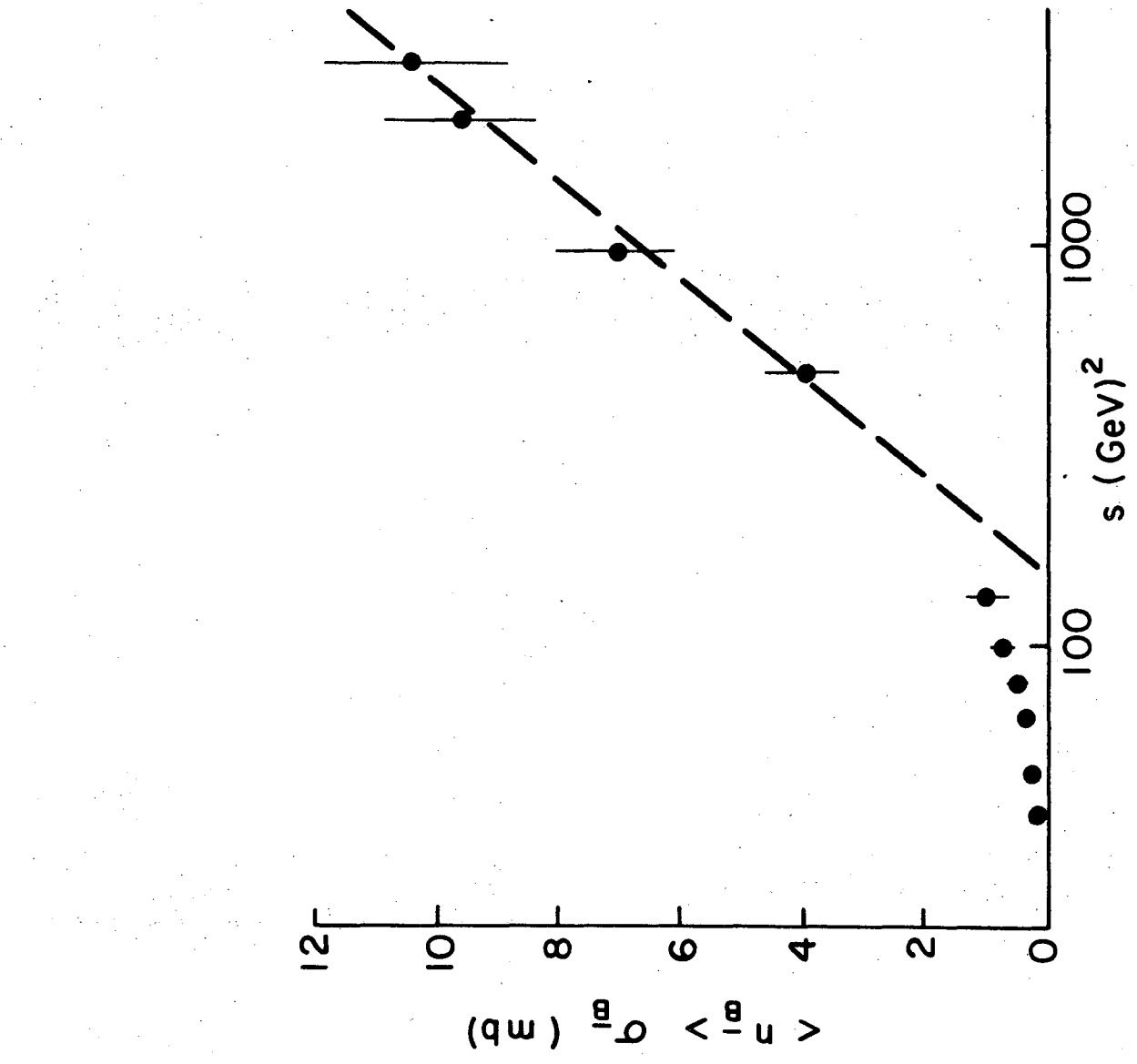
$\langle n_{el} \rangle \sigma_{el}$ (mb)
0
2
4
6
8
10
12
100
1000
s (GeV)^2
XBL744-2939

Fig. 1

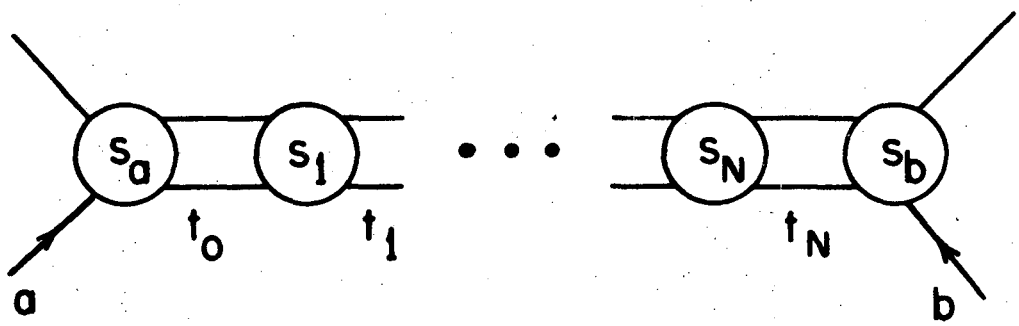

XBL744-2934

Fig. 2.1

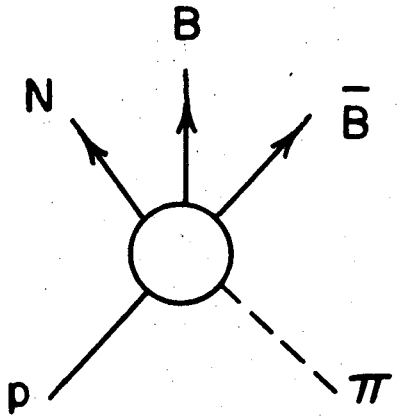

(a)

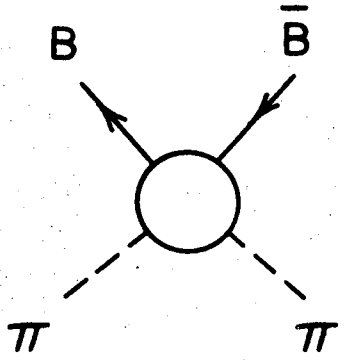

(b)

XBL744-2935

Fig. 2.2

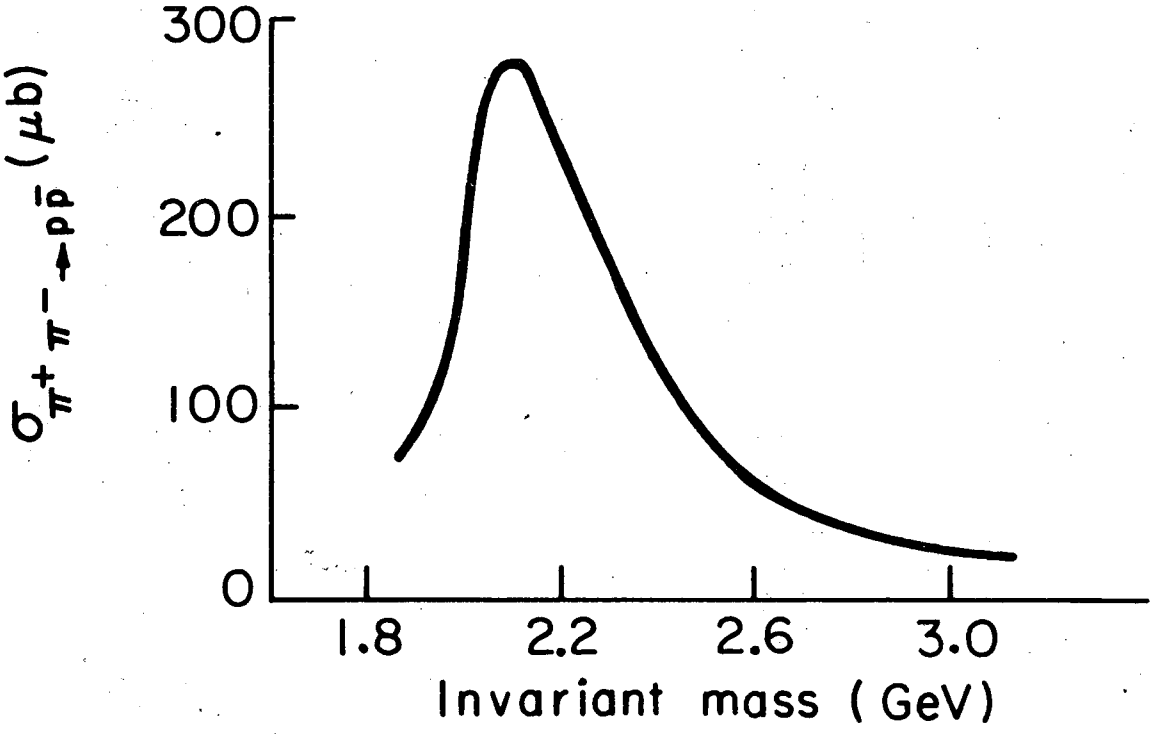

XBL744-2955

Fig. 2.3

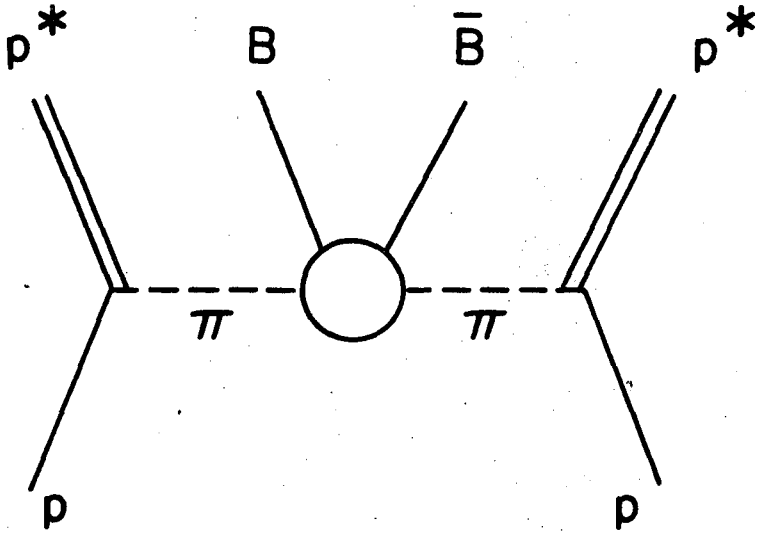

XBL744-2933

Fig. 2.4

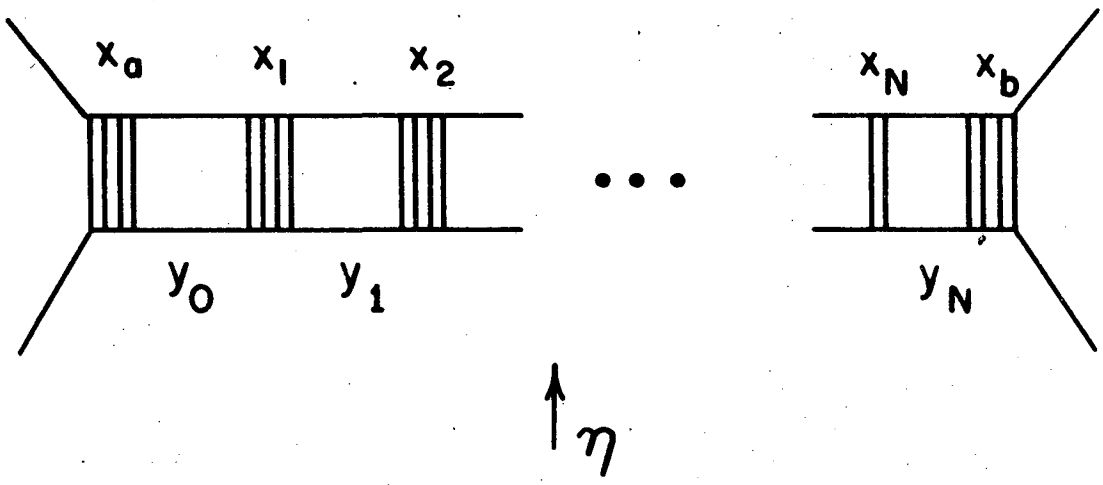

XBL744-2942

Fig. 3.1

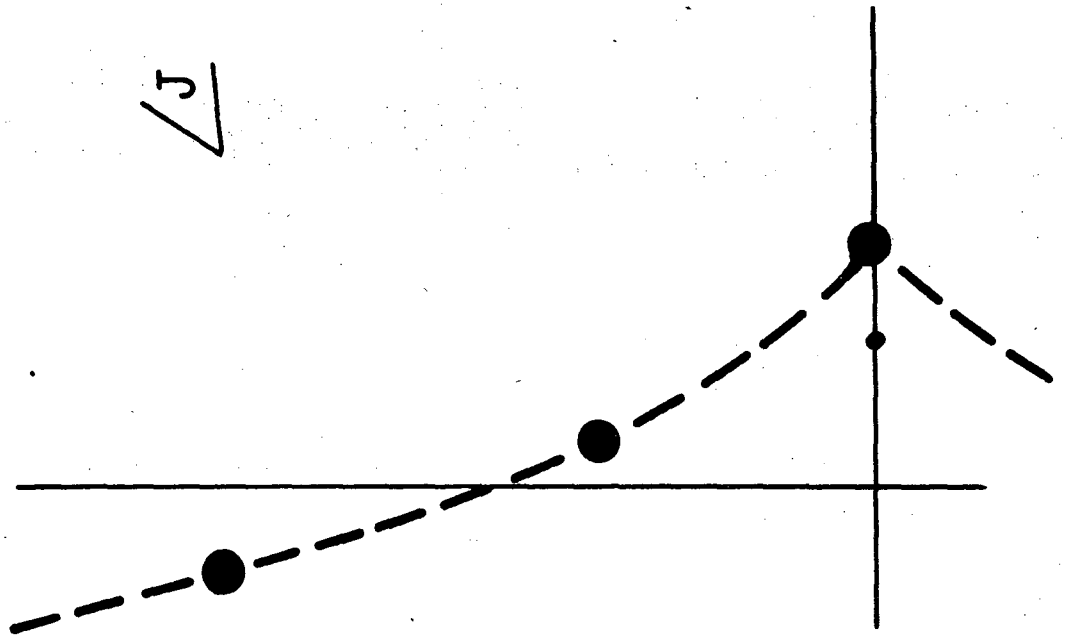

XBL744-2952

Fig. 3.2

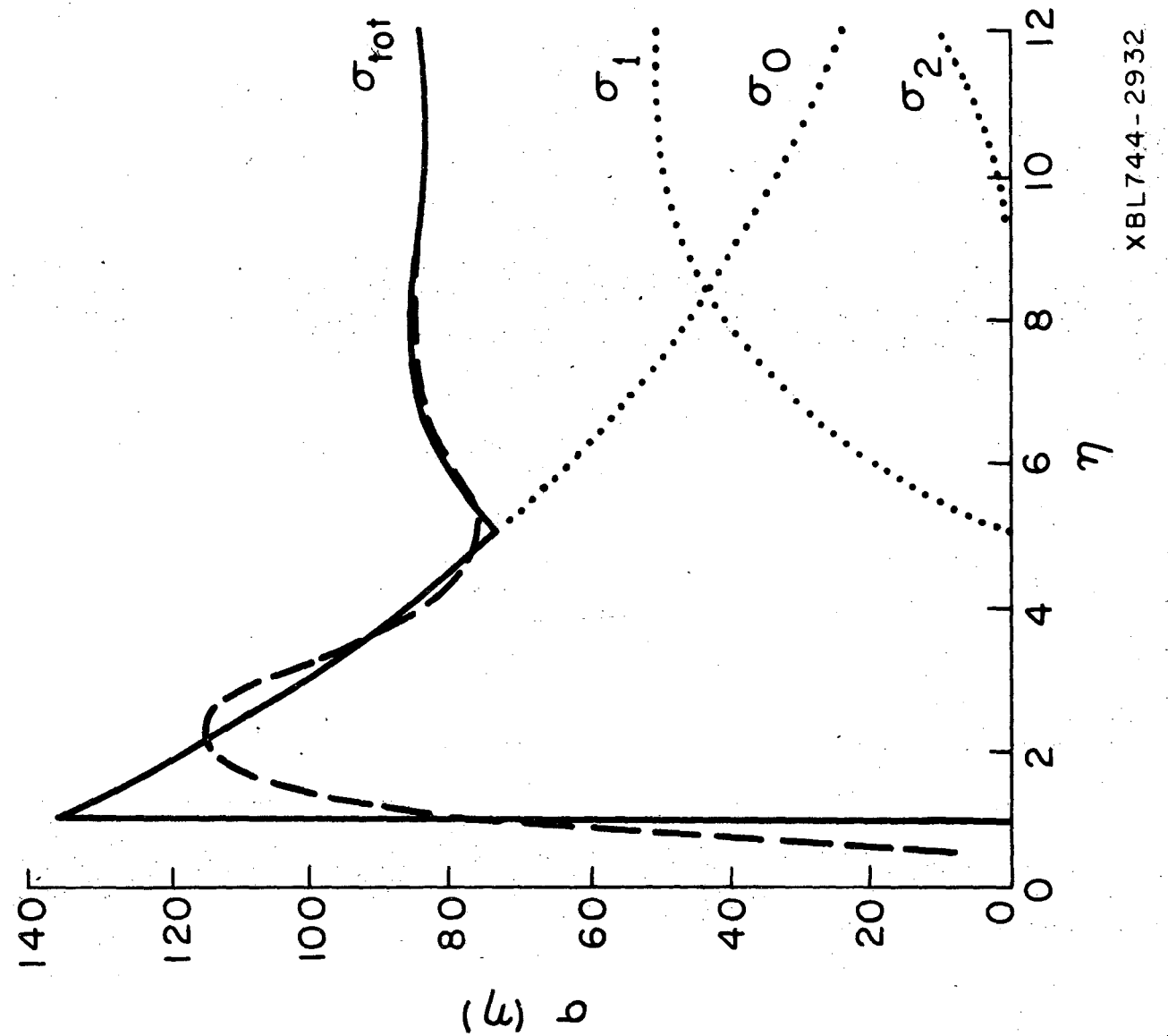
σ tot
σ 1
σ 0
σ 2
σ (η)
η
0
20
40
60
80
100
120
140
0
2
4
6
8
10
12
XBL744-2932

Fig. 3.3

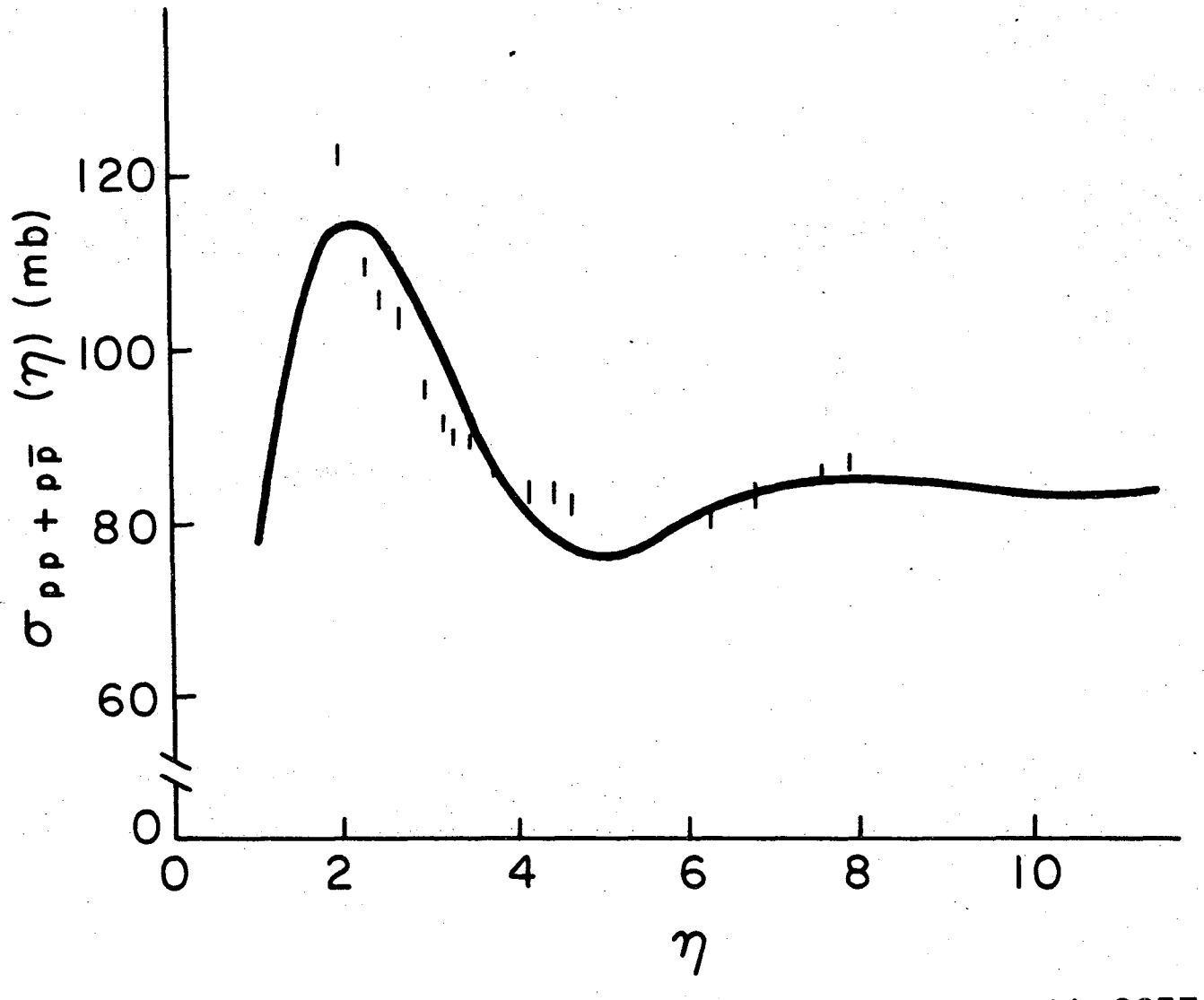

Fig. 3.4

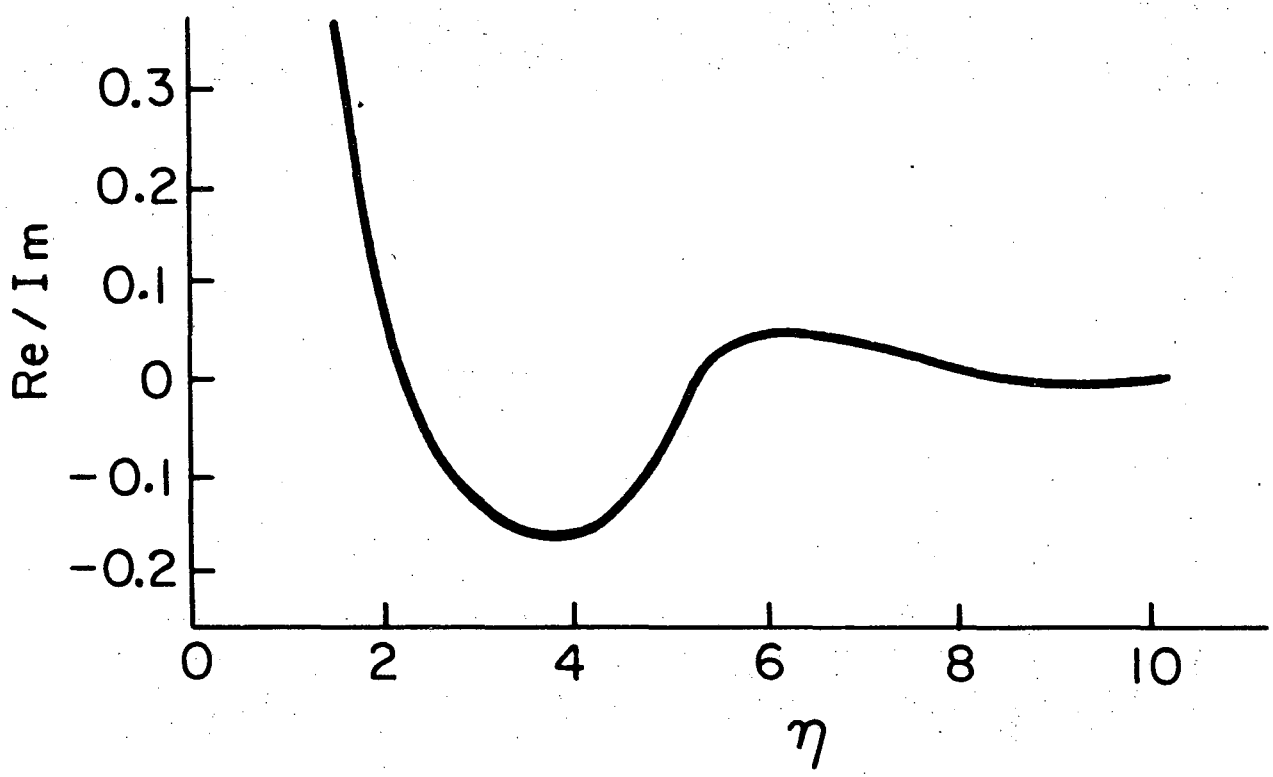

Fig. 3.5

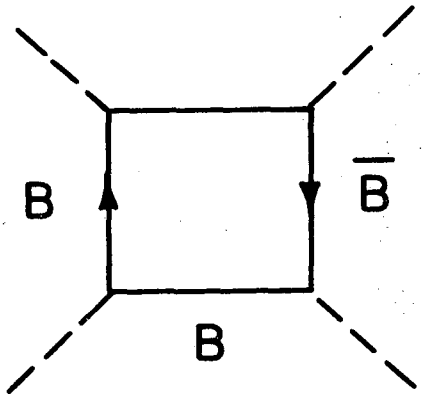

XBL744-2954

Fig. 3.6

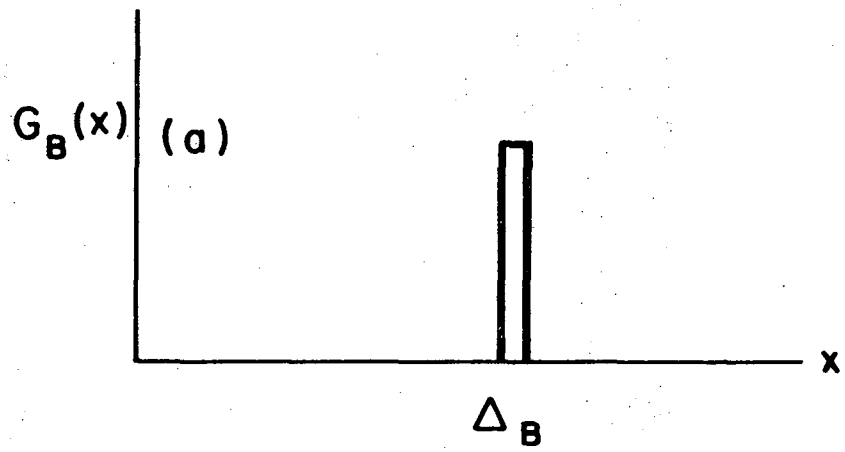

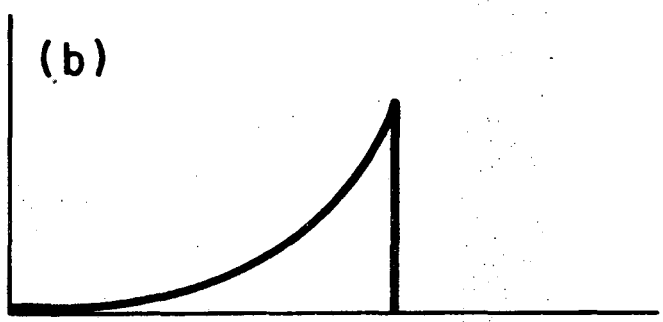

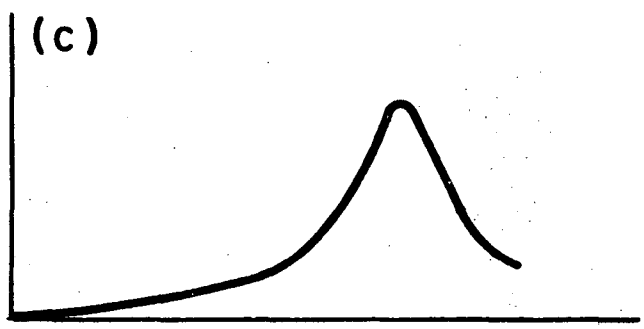

XBL744-2943

Fig. 4.1

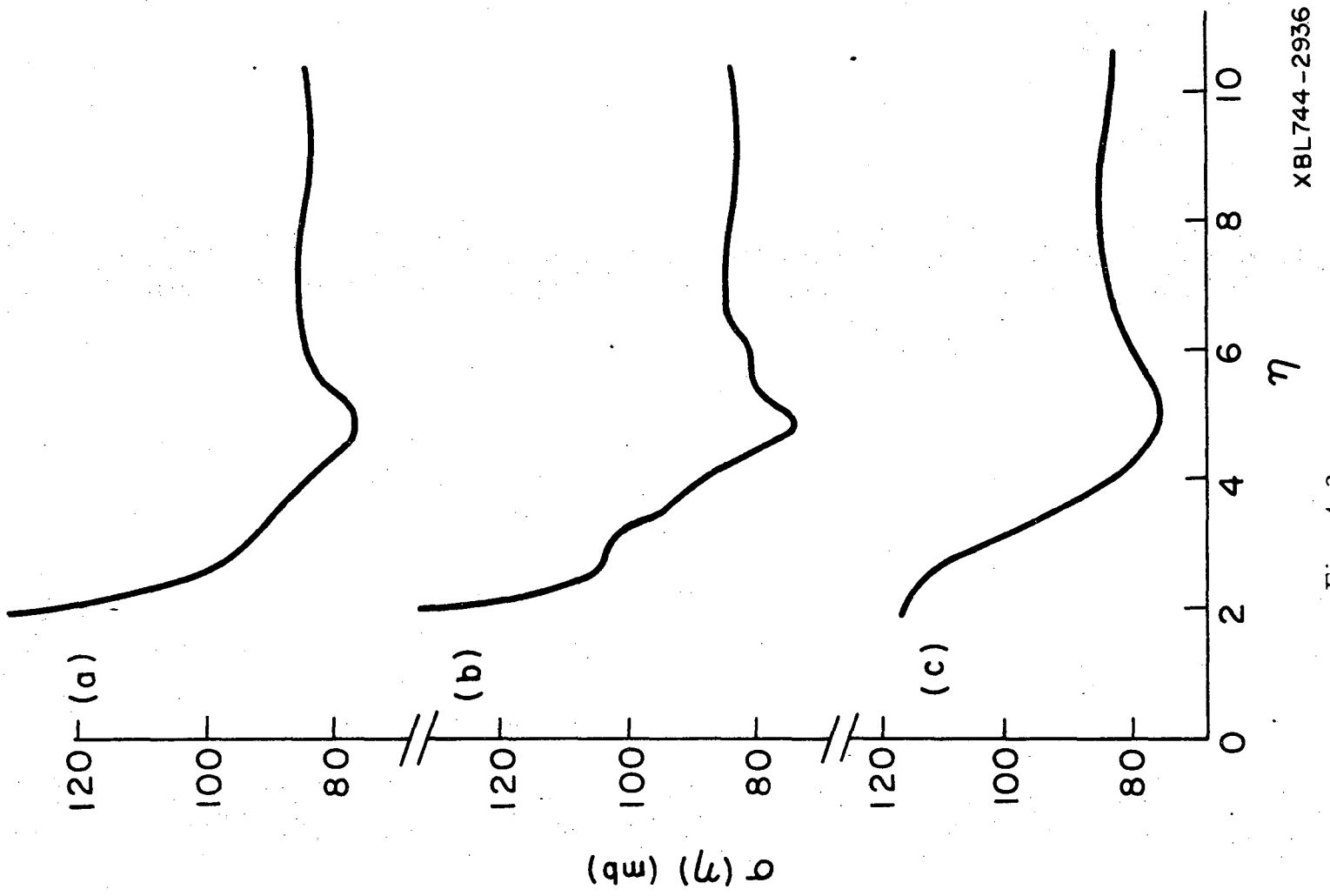

Fig. 4.2

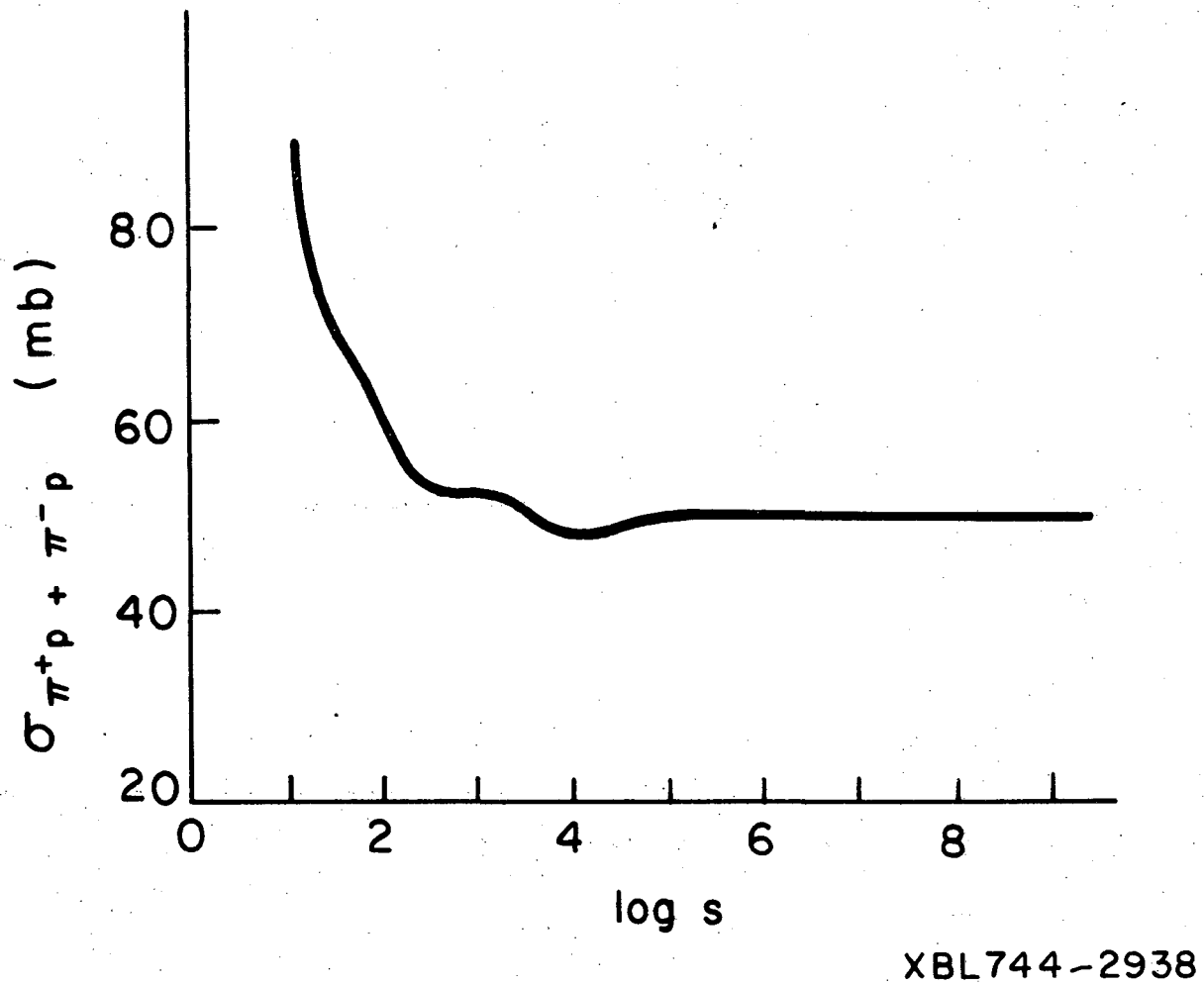

Fig. 4.3

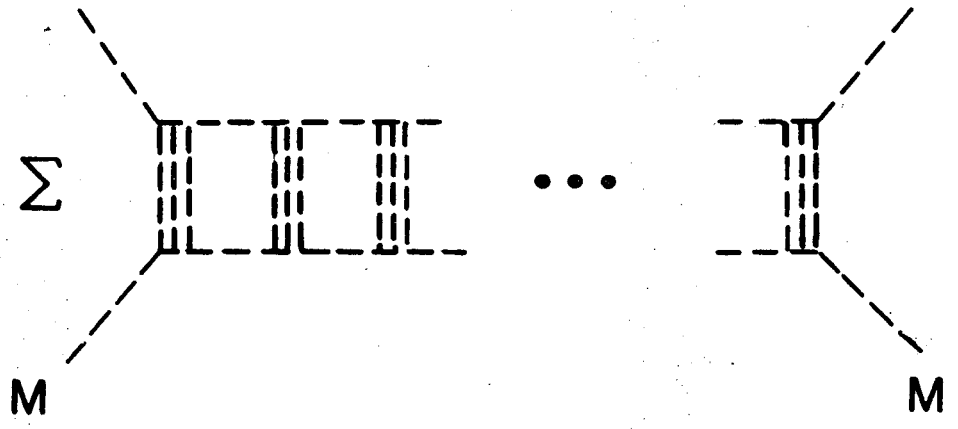

XBL744-2941

Fig. 5.1

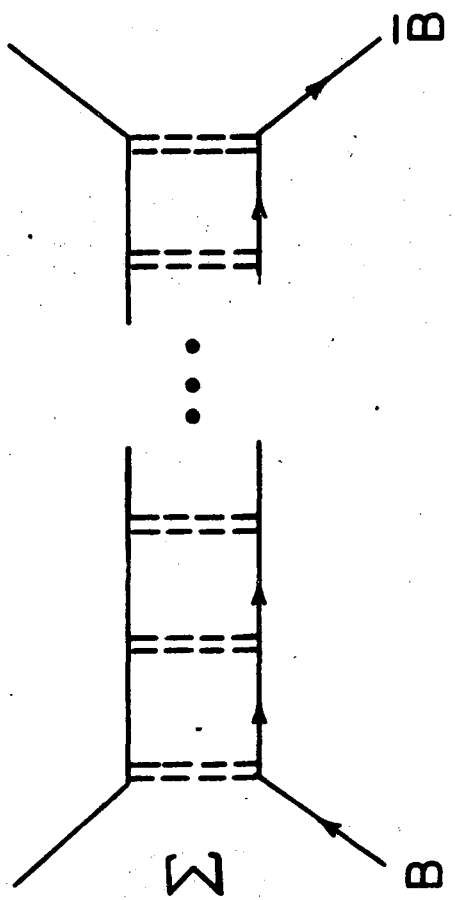

XBL744-2940

Fig. 5.2

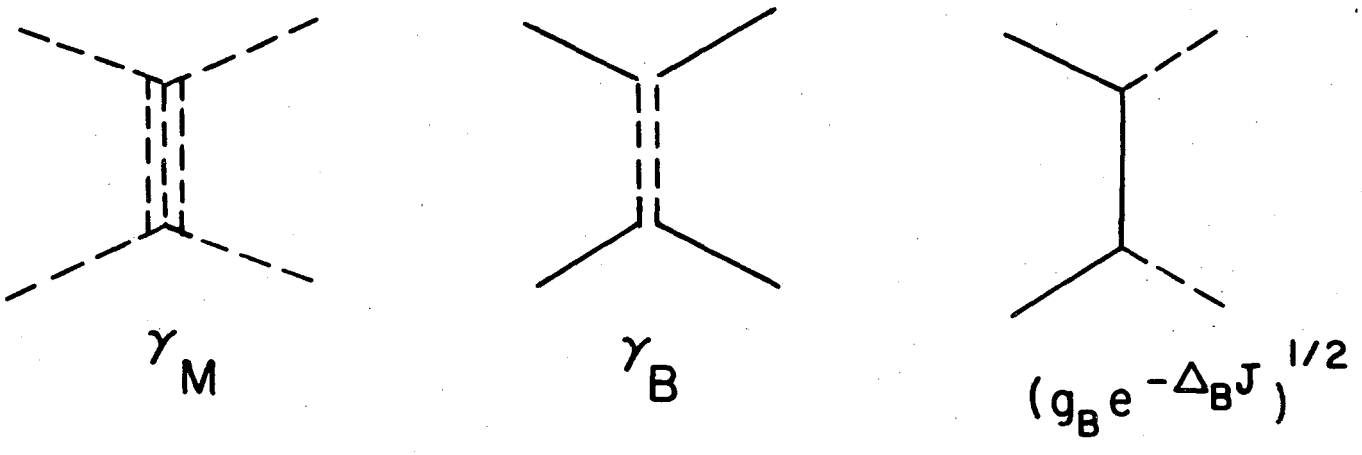

Fig. 5.3

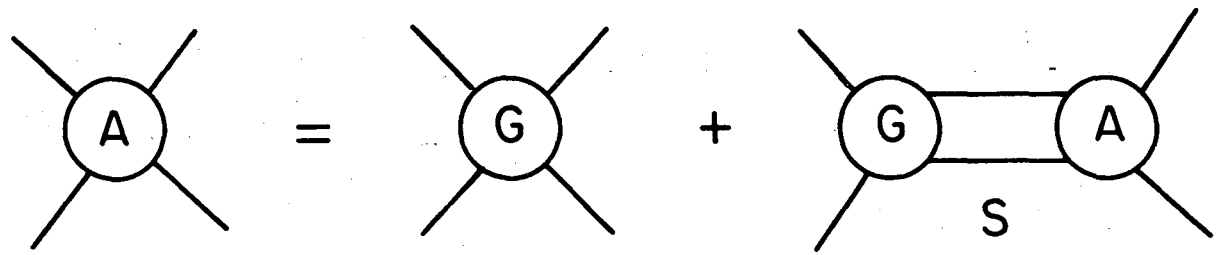

XBL744-2950

Fig. 5.4

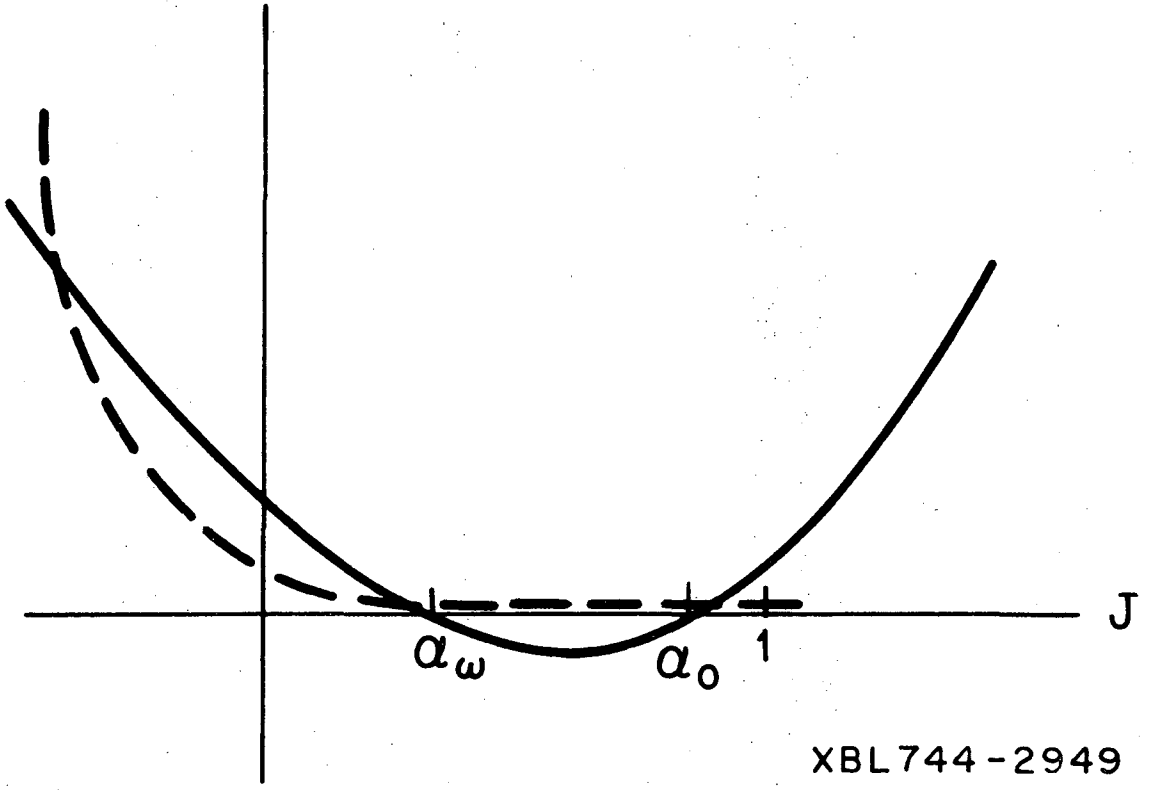

Fig. 5.5

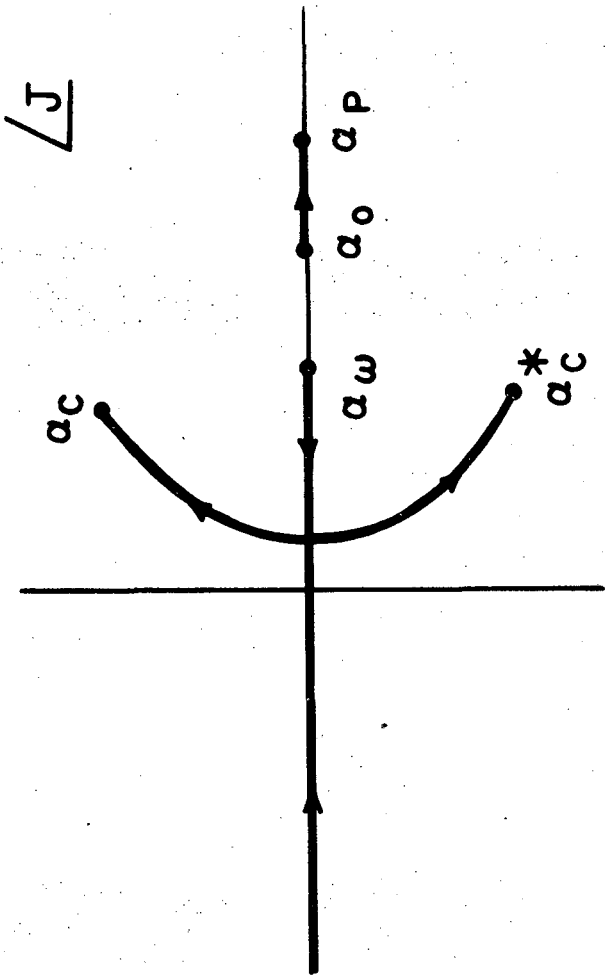

Fig. 5.6

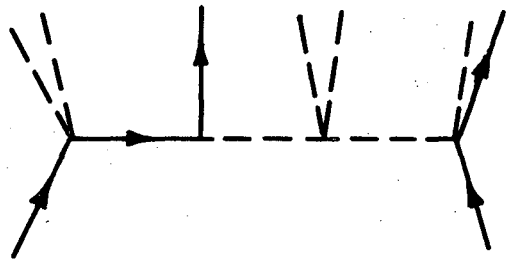

XBL744-2947

Fig. 5.7

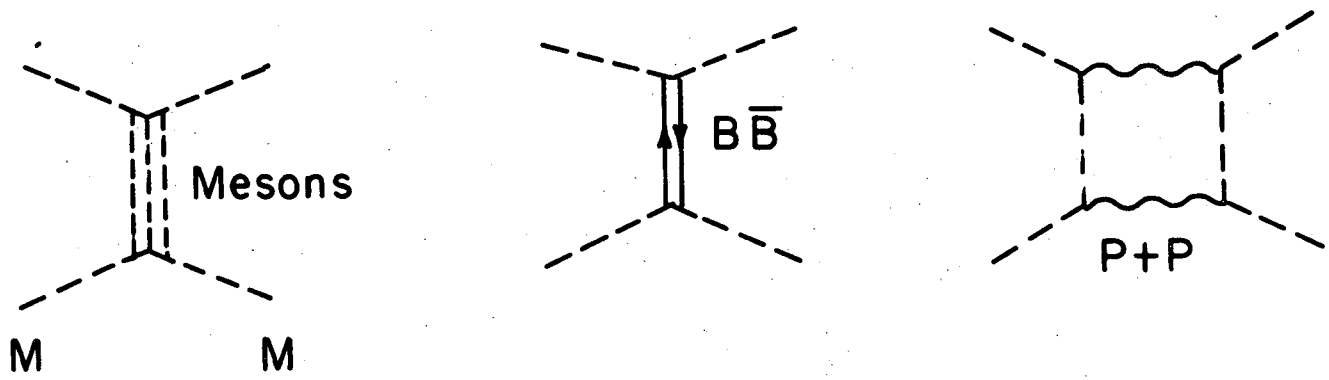

XBL744-2946

Fig. 6.1

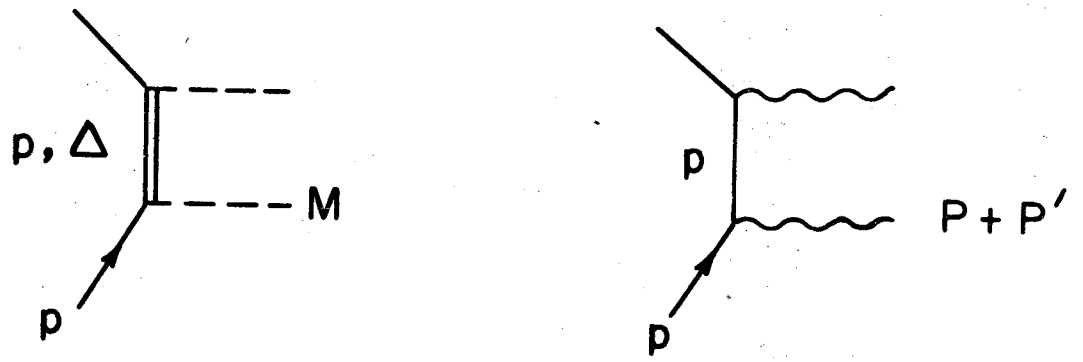

XBL744-2945

Fig. 6.2

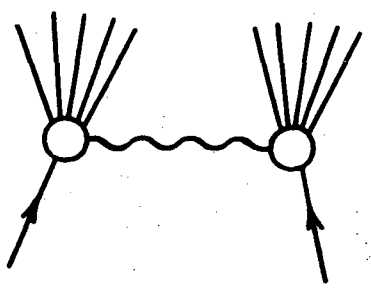

(a)

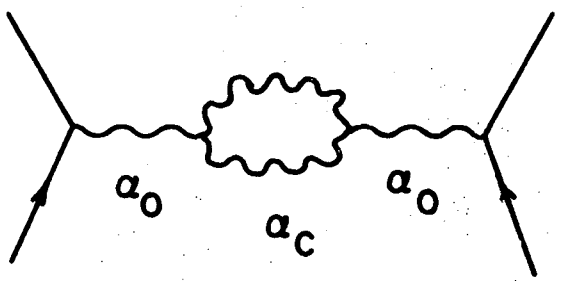

(b)

XBL744-2944

Fig. A.1

TECHNICAL INFORMATION DIVISION
LAWRENCE BERKELEY LABORATORY
UNIVERSITY OF CALIFORNIA
BERKELEY, CALIFORNIA 94720